

# Exponential self-similar mixing by incompressible flows

GIOVANNI ALBERTI, GIANLUCA CRIPPA, ANNA L. MAZZUCATO

*Dedicated to Alberto Bressan and Charles R. Doering on the occasion of their 60<sup>th</sup> birthdays*

**ABSTRACT.** We study the problem of the optimal mixing of a passive scalar under the action of an incompressible flow in two space dimensions. The scalar solves the continuity equation with a divergence-free velocity field which satisfies a bound in the Sobolev space  $W^{s,p}$ , where  $s \geq 0$  and  $1 \leq p \leq \infty$ . The mixing properties are given in terms of a characteristic length scale, called the mixing scale. We consider two notions of mixing scale, one functional, expressed in terms of the homogeneous Sobolev norm  $\dot{H}^{-1}$ , the other geometric, related to rearrangements of sets. We study rates of decay in time of both scales under self-similar mixing. For the case  $s = 1$  and  $1 \leq p \leq \infty$  (including the Lipschitz case, and the case of physical interest of enstrophy-constrained flows), we present examples of velocity fields and initial configurations for the scalar that saturate the exponential lower bound established in previous works for the decay in time of both scales. We also present several consequences for the geometry of regular Lagrangian flows associated to Sobolev velocity fields.

**KEYWORDS:** mixing, continuity equation, negative Sobolev norms, incompressible flows, self-similarity, potentials, regular Lagrangian flows.

MSC (2010): 35Q35, 76F25

## CONTENTS

1. Introduction	3
1.1. The continuity equation	3
1.2. Functional and geometric mixing scales	4
1.3. Main results	5
1.5. Past literature	6
1.6. Self-similarity ansatz and structure of our constructions	8
1.7. Further remarks and open problems	9
1.8. Geometry of regular Lagrangian flows	10
1.9. Follow up: loss of regularity for continuity equations	11
Acknowledgements	11
2. Preliminaries	11
2.1. Homogeneous Sobolev spaces $\dot{H}^s$	12
2.3. Homogeneous Sobolev spaces $\dot{W}^{s,p}$	13
2.5. Lipschitz-Hölder spaces	14

---

2.7. Scaling properties	14
2.9. Interpolation	14
2.10. Definition. Functional mixing scale [31, 36]	15
2.11. Definition. Geometric mixing scale [13]	15
3. Scaling analysis in a self-similar construction	15
3.1. Assumption. Self-similar base element	16
3.3. A self-similar construction	16
3.6. Regularity in time	19
4. First geometric construction	19
4.1. Paths and curves	20
4.2. Time-dependent paths and curves	20
4.3. Time-dependent domains	21
4.4. Compatible velocity fields	21
4.8. Homothetic curves	23
4.11. Potential of a velocity field	24
5. First example: pinching	26
6. Scaling analysis in a quasi self-similar construction	29
6.1. Assumption. Almost self-similar basic family	29
6.2. Quasi self-similar construction	30
6.3. Assumption. Regularity of the patching	31
6.6. Decay of the functional mixing norm	33
6.9. A combinatorial construction	35
7. Second geometric construction	36
7.4. Canonical velocity field associated to a time-dependent curve	39
7.5. Canonical solution associated to a time-dependent curve	39
7.7. Centered sub-arcs and curved rectangles	40
8. Second example: Peano snake	42
8.1. Quasi self-similar basic curves: conditions	42
8.2. Explanation of the combinatorics	42
8.3. Reduction: simplified geometric conditions	43
8.5. Construction of velocity fields and solutions	44
8.6. Verification of Assumption 6.1	45
8.7. Verification of Assumption 6.3	45
8.8. Regularity in space of solutions	46
8.9. Regularity in time of velocity fields and solutions	46
8.10. Construction of $\Gamma_1$ and $\Gamma_2$ for $t = 0, t = 1$	47
8.11. Construction of $\Gamma_1(t)$ for $0 < t < 1$	47
8.12. Construction of $\Gamma_2(t)$ for $0 < t < 1$	48
References	49

## 1. INTRODUCTION

We study the problem of optimal mixing of scalar, passive tracers by incompressible flows. How well a quantity transported by a flow is mixed is an important problem in fluid mechanics and in many applied fields, for instance in atmospheric and oceanographic science, in biology, and in chemistry. In combustion, for example, fuel and air need to be well mixed for an efficient reaction to take place. In many situations, the interaction between the tracer and the flow can be neglected: mathematically, this results in the fact that the tracer solves a linear continuity equation with a given velocity field (see (1.1)). This problem is also a surprisingly rich source of questions in analysis, relating partial differential equations and dynamical systems with geometric measure theory in particular.

There is a well-established fluid mechanics literature concerning mixing and turbulence, especially with respect to statistical properties (see e.g. [11, 22] and references therein). It is known, in fact, that turbulent advection enhances mixing, which in turn can enhance diffusion and suppress concentration (see [15] for steady “relaxation enhancing” flows and [29] for an application to chemotaxis, for instance). Enhanced dissipation occurs also in Euler flows as an effect of inviscid Landau damping (see [9] and references therein). Mixing has also long been studied in the context of chaotic dynamics [7, 37, 33]. Indeed the decay to zero of the mixing scale defined in terms of negative Sobolev norms corresponds to ergodic mixing by the flow (as shown in [35]), and several well-known examples of discrete dynamical systems exhibit an exponential decay of correlations, which essentially means exponential mixing (however, these examples cannot be easily adapted to our context).

Recently there has been a renewed interest in quantifying the degree of mixing under an incompressible flow, and in producing examples that achieve optimal mixing. On the analytical side, progress has been possible in part due to the development of new tools to study transport and continuity equations under non-Lipschitz velocities [20, 5, 6], in particular quantitative estimates on regular Lagrangian flows [16]. On the applied and computational side, optimal mixing has been approached from the point of view of homogenization and control with more realistic models [32, 21]. More accurate experiments have also been performed (see for example [23, 28, 27]).

**1.1. The continuity equation.** We consider the two-dimensional setting, as it is the first dimension with non-trivial divergence-free velocity fields and for comparison with computational and experimental studies. Generally, dimension will not play a crucial role if what follows, except in setting scaling laws. The divergence-free condition is a strong constraint that can be somewhat relaxed, but it is physically motivated in applications of mixing. In fact, since we aim at producing examples of optimal mixing, the divergence-free condition is a more restrictive requirement that must be satisfied in our constructions.

We work on the two-dimensional torus  $\mathbb{T}^2 := \mathbb{R}^2/\mathbb{Z}^2$  or on the plane  $\mathbb{R}^2$ . When considering the plane  $\mathbb{R}^2$ , both velocity fields and solutions eventually resulting from our constructions will be supported in a fixed compact set.

Given a divergence-free, time-dependent velocity field  $u = u(t, x)$ , we consider a passive scalar  $\rho = \rho(t, x) \in L^\infty$  which is advected by  $u$ , i.e., a solution of the continuity equation

$$\partial_t \rho + \operatorname{div}(u\rho) = 0, \quad (1.1)$$

with prescribed initial datum  $\rho(0, \cdot) = \bar{\rho}$  at time  $t = 0$ .

We always assume without loss of generality<sup>1</sup> that the initial datum  $\bar{\rho}$  satisfies the zero-average condition  $\int \bar{\rho} = 0$ , where the integration is performed over  $\mathbb{T}^2$  or over  $\mathbb{R}^2$ , depending on the case under consideration. Since the continuity equation (1.1) preserves the total integral of the solution along the time evolution, it follows that  $\rho(t, \cdot)$  has average zero for any time  $t$  (this is relevant in connection with the measurement of the mixing scale with negative Sobolev norms, see Definition 2.10, §2.1, and Remark 2.2). This assumption is also physically consistent with  $\rho$  representing a tracer.

**1.2. Functional and geometric mixing scales.** In order to discuss the mixing properties of solutions to the continuity equation (1.1) we need to define a notion of mixing scale, which can give a quantification of the “level of mixedness” of the solution  $\rho(t, \cdot)$  at time  $t$ . The continuity equation preserves (formally at least) all  $L^p$  norms of the solution.<sup>2</sup> Though, it is still possible for  $\rho(t, \cdot)$  to converge to zero weakly.<sup>3</sup> In fact, the vanishing of the homogeneous negative Sobolev norm  $\dot{H}^{-1}$  of  $\rho(t, \cdot)$  (see §2.1 for its definition) can be proved to be equivalent to the convergence of  $\rho(t, \cdot)$  to 0 weakly in  $L^2$  (see for instance [31]). More generally, the use of negative norms to measure mixing was proposed in [36], where the equivalence between the decay of the  $\dot{H}^{-1/2}$  norm and mixing in the ergodic sense was established.

In this paper, we will employ and compare two notions of mixing scales that are considered in the literature. The first one is based on a negative Sobolev norm of the solution  $\rho(t, \cdot)$ , more precisely the norm in the homogeneous Sobolev space  $\dot{H}^{-1}$  following [31] (see Definition 2.10 below), and will be referred to as the *functional mixing scale*.<sup>4</sup> The second mixing scale arises from a conjecture of

<sup>1</sup> It is enough to subtract to the solution its total integral, and observe that constants are solutions of (1.1).

<sup>2</sup> In fact,  $L^p$  norms of the solutions are frequently used as a measurement of the mixing scale for solutions of advection-diffusion equations, i.e., in the case when  $\rho$  solves  $\partial_t \rho + \operatorname{div}(u\rho) = \Delta \rho$ . Due to the viscosity,  $L^p$  norms of the solution are dissipated along the time evolution.

<sup>3</sup> Using characteristic functions of sets as test functions, it is not difficult to prove that this will be the case for instance if the flow of  $u$  is strongly mixing in the ergodic sense.

<sup>4</sup> From a mathematical point of view there is nothing special with the order  $-1$  that has been chosen in the definition of functional mixing scale: every negative Sobolev norm would behave in a similar way. However, from a physical point of view, this choice is the most convenient, since the norm in  $\dot{H}^{-1}$  scales as a length.

Bressan [13] on the cost of rearrangements of sets and brings in a connection with geometric measure theory. This second notion of scale is expressed in terms of the relative proportion in suitably small balls of different level sets of the solution (see Definition 2.11 below), and it will be referred to as the *geometric mixing scale*. The two scales are related though generally not equivalent.

In the next few paragraphs in this introduction, we *informally* denote any of the two mixing scales of the solution at time  $t$  by  $\text{mix}(\rho(t, \cdot))$ .

Ideally, a flow that “mixes optimally” will achieve the largest decay rate in time for  $\text{mix}(\rho(t, \cdot))$ . How fast  $\text{mix}(\rho(t, \cdot))$  can decay in time depends on properties of the flow. These, in turn, are in practice given in terms of constraints on certain quantities of physical interest, typically energy, enstrophy, and palenstrophy. These correspond respectively to uniform-in-time bounds on the  $L^2$ ,  $H^1$ , and  $H^2$  norms of the velocity field  $u$ .

**1.3. Main results.** In this article, we provide explicit examples of two-dimensional flows that mix certain configurations optimally under a fixed enstrophy budget. In fact, more generally our work gives examples of optimal mixers under a constraint on the Sobolev norm  $W^{1,p}$  of the velocity field, where  $1 \leq p \leq \infty$ , i.e., the Lipschitz case is included.

As described in detail in §1.5 below, under uniform in time constraints on the Sobolev norm  $W^{1,p}$  of the velocity field, where  $1 < p \leq \infty$ , it has been recently proved [16, 25, 39] that the (functional or geometric) mixing scale can decay at most exponentially in time:

$$\text{mix}(\rho(t, \cdot)) \geq C \exp(-ct), \quad (1.2)$$

where  $C > 0$  and  $c > 0$  are constant depending on the initial datum  $\bar{\rho}$  and on the given bounds on the velocity field. The optimality of this bound in the full range of summability exponents was previously unknown (see however [41] and the brief description in §1.5 below).

Our main results are contained<sup>5</sup> in Theorem 3.4 and Theorem 6.7 and can be summarized as follows:

*There exist a smooth, bounded, divergence-free velocity field  $u$ , which is Lipschitz uniformly in time, and a bounded nontrivial solution  $\rho$  of the continuity equation (1.1), such that the (functional or geometric) mixing scale of the solution decays exponentially in time:*

$$\text{mix}(\rho(t, \cdot)) \leq C \exp(-ct), \quad (1.3)$$

*which shows the optimality of the lower bound (1.2).*

**Remark 1.4.** (i) The optimal decay in (1.3) holds for both the functional and the geometric mixing scales.

---

<sup>5</sup> The verification of the assumption of the two theorems is carried on in Sections 5 and 8 respectively.

(ii) The solution  $\rho$  can be required to be smooth, or to be the characteristic function of a set which evolves in time under the action of the flow.

(iii) Our procedure extends to a full scaling analysis: if the velocity field is required to be bounded in  $W^{s,p}$  uniformly in time, for some  $s \geq 0$  real, then the constructed  $u$  and  $\rho$  are such that:

- If  $s < 1$  there is a time  $t^*$  such that  $\text{mix}(\rho(t^*, \cdot)) = 0$ , i.e., there is perfect mixing in finite time;
- If  $s = 1$  the exponential decay of the mixing scale in (1.3) holds;
- If  $s > 1$  there is polynomial decay of the mixing scale: there exists an exponent  $\alpha = \alpha(s) > 0$  such that  $\text{mix}(\rho(t, \cdot)) \leq Ct^{-\alpha}$ .

(iv) It is very important to keep in mind the difference between the regularity of the velocity field, and the regularity bounds that it satisfies uniformly in time. For instance, in the situation with exponential decay of the mixing scale of the solution sketched in §1.3, the velocity field is smooth in space and time; however, only Sobolev norms  $W^{s,p}$  with  $0 \leq s \leq 1$  and  $1 \leq p \leq \infty$  are bounded uniformly in time. If  $s > 1$ , such norms are bounded for every given  $t$ , but blow up when  $t \rightarrow \infty$ .<sup>6</sup>

Further remarks are detailed in §1.6 and §1.7 below. The results presented in this article were announced in [4].

Before making further observations on our results and techniques we make a digression about the past literature on this topic.

**1.5. Past literature.** Mixing phenomena are studied in the literature under energetic constraints on the velocity field, that is, assuming that the velocity field is bounded with respect to some spatial norm, uniformly in time. This research area is related in a very natural way to the study of transport and continuity equations under non-Lipschitz velocities (see [6] for a recent survey of this research area). We now make an overview of some previous works on these topics (most of the results hold indeed in any space dimension):

- (a) The velocity field  $u$  is bounded in  $W^{s,p}$  uniformly in time for some  $s < 1$  and  $1 \leq p \leq \infty$  (the case  $s = 0$ ,  $p = 2$ , relevant for the applications, is often referred to as energy-constrained flow). In this case, there is in general no uniqueness for the Cauchy problem for the continuity equation (1.1) (see [2, 1]). Hence, one can find a velocity field and a bounded solution which is non-zero at the initial time, but is identically zero at some later time. Therefore it is possible to have perfect mixing in finite time, as already observed in [31] and established in [34] for  $s = 0$ , building on an example from [18, 13].
- (b) The velocity field  $u$  is bounded in  $W^{1,p}$  uniformly in time for some  $1 \leq p \leq \infty$  (the case  $p = 2$ , relevant for the applications, is often referred to as enstrophy-constrained flow). The theory in [20] guarantees uniqueness for the Cauchy problem (1.1), which in particular excludes perfect mixing in

<sup>6</sup> In formulas, we have that  $u \in L^\infty([0, +\infty); W^{s,p}(\mathbb{R}^2))$  if and only if  $0 \leq s \leq 1$ .

finite time. A quantification of the maximal decay rate for the mixing scale has been achieved thanks to the quantitative Lipschitz estimates for regular Lagrangian flows in [16]. In detail, for  $p > 1$ , the theory in [16] provides an exponential lower bound on the geometric mixing scale (see (1.2)). The extension to the borderline case  $p = 1$  is still open (see, however, [12]). The same exponential lower bound (1.2) has been proved for the functional mixing scale in [25, 39]. A new proof of these lower bounds based on harmonic analysis estimates has been proposed in [30].

- (c) The theory in [5] provides uniqueness for the Cauchy problem (1.1) for velocity fields bounded in  $BV$  uniformly in time. Again, this excludes perfect mixing in finite time. The validity of the bound (1.2) is still unknown in this context. However, in [13] it is observed that such an exponential decay of the geometric mixing scale can indeed be attained for velocity fields bounded in  $BV$  uniformly in time. Actually, the same example works also for the functional mixing scale.
- (d) The velocity field  $u$  is bounded in  $W^{s,p}$  uniformly in time for some  $s > 1$  and  $1 \leq p \leq \infty$  (the case  $s = 2$  and  $p = 2$ , relevant for the applications, goes under the name of palenstrophy-constrained flow). No better bounds for the decay of the (functional or geometric) mixing scale than (1.2) are known. The common belief, supported also by the numerical simulations in [34, 25], is that this bound is optimal. See also the discussion in §1.7.

Besides depending on the given bounds on the velocity field, the constants  $C$  and  $c$  in (1.2) depend on the initial datum  $\bar{\rho}$ , and not only on its mixing scale. In fact, even for the functional mixing scale, it is not clear that an estimate of the form

$$\|\bar{\rho}(t, \cdot)\|_{\dot{H}^{-1}} \geq C \|\bar{\rho}\|_{\dot{H}^{-1}} \exp(-ct),$$

with  $C$  and  $c$  universal constants depending only on the given bounds on the velocity field, can be achieved. It is then natural to ask whether it is possible to obtain bounds on the rate of decay with constants that only depend on the mixing scale of the initial tracer configuration, and not on its geometry. Unfortunately, direct PDE methods, such as energy estimate, do not seem to yield sharp bounds. For instance, they yields a Gaussian bound for palenstrophy-constrained flows, when the optimal bound is at least exponential (see [34]).

Besides the examples constructed in the present article (§1.3), there are other explicit examples in the literature of flows that saturate the exponential decay rate for enstrophy-constrained flows. Yao and Zlatoš [41] utilize a cellular flow to establish exponential mixing for any bounded solution and with a bound on the  $W^{1,p}$ -norm of the velocity field in the range  $1 \leq p \leq \bar{p}$  for some  $\bar{p} > 2$ . They also give an interesting result on “unmixing” a given configuration. See also §1.7 for a comparison of our results with those from [41].

Before these analytical results, several numerical experiments have been performed, that supported an exponential rate of decay for  $\text{mix}(\rho(t, \cdot))$  under an

enstrophy budget. For instance, in [31] a flow that instantaneously maximizes the rate of decay of the mixing scale for a sinusoidal initial configuration of the passive scalar was displayed. A global optimizer was computed numerically in [35].

**1.6. Self-similarity ansatz and structure of our constructions.** In order to implement our constructions of optimal mixers we follow a self-similar scheme. In few words, we assume that the solution undergoes (on a suitable time scale) an evolution that is constructed starting from a basic move and then successively rescaling this move on finer and finer spatial scales (the reader can glimpse at this construction in Figure 1).

A few comments are in order. We assume the self-similarity as an ansatz for our examples. We do not claim that a self-similar evolution is more physical<sup>7</sup> or more mixing-optimizing than other evolutions. We consider self-similar evolutions since this choice has the substantial advantage of making computations rather easy: given the existence of the basic move, all estimates for the evolution can be derived through a fairly simple scaling analysis. The difficulty is of course proving the existence of the basic move within the required regularity setting.

Following this line of thinking, our analysis contains three main stages:

- (1) Scaling analysis: the existence of a basic move for time  $0 \leq t \leq 1$  being assumed, we define the evolution for all times  $t \geq 0$  and fully characterize the decay of the mixing scale of the solution and the energetic constraints on the velocity field (Section 3);
- (2) Geometric tools: we establish a series of geometric lemmas that guarantee the existence of smooth, divergence-free velocity fields with the property that the associated flows deform smooth sets according to a prescribed evolution in time (Section 4);
- (3) Existence of the basic move: we use such geometric tools to construct the basic move (that is, we construct the velocity field and a weak solution of the continuity equation, the level sets of which realize the geometric evolution). The main technical point here is to deal with the singularities that are present in the evolution. This last stage “validates” the scaling analysis in (1) (Section 5).

We notice that, although self-similarity can be quite a rigid constraint, the decay in time of the mixing scale of an enstrophy-constrained self-similar evolution matches the known exponential lower bound (recall (1.3) and §1.5(b)). This is not the case in the context of palenstrophy-constrained flows, where the rate of decay ensuing from self-similar evolution is polynomial in time, rather than the observed exponential rate (recall §1.5(d)).

One shortcoming of the strategy based on self-similarity is the limited regularity available for velocity field and solution. In Section 5, the velocity field cannot have

---

<sup>7</sup> Mixing patterns with decaying amplitude but invariant geometrical structure have been experimentally observed [38].



Lipschitz regularity and the solution is a characteristic function of a set evolving in time.

In order to overcome this problem, we introduce in Section 6 the notion of quasi self-similar evolution. Instead of replicating rescaled copies of one basic element at each step of the evolution, we rather consider a finite family of basic elements, which are rescaled and rearranged at each step of the evolution according to a combinatorial pattern (the reader can glimpse at this construction in Figures 5 and 6). In Sections 6, 7, and 8 we follow the same line of work described in (1)–(2)–(3) above: we perform a scaling analysis under the condition that a finite family of basic moves exists, we develop geometric tools well suited to deform smooth profiles, and eventually we use such tools to construct the family of the basic moves. In this way, we are able to obtain a velocity field and an associated solution of the continuity equation that are actually smooth.

**1.7. Further remarks and open problems.** Our main result is a proof of the optimality of (1.2). In order to do this, we construct one velocity field, which is bounded in  $W^{1,p}$  uniformly in time for any  $1 \leq p \leq \infty$ , and one solution, whose mixing scale decays exponentially. In fact, with our strategy it is possible to construct a large class of initial data whose mixing scale decays exponentially. However, it is unclear whether this is the case for every initial datum. The following questions about the existence of “universal mixers” are therefore very natural.

- (a) Given a bounded initial datum  $\bar{\rho}$ , does it exist a velocity field, bounded in  $W^{1,p}$  uniformly in time and possibly dependent on  $\bar{\rho}$ , such that  $\text{mix}(\rho(t, \cdot))$  decays to zero?
- (b) If the answer to Question (a) is positive, does it exist a velocity field, bounded in  $W^{1,p}$  uniformly in time, such that the decay to zero of  $\text{mix}(\rho(t, \cdot))$  is precisely exponential?
- (c) Does it exist a velocity field, bounded in  $W^{1,p}$  uniformly in time, such that  $\text{mix}(\rho(t, \cdot))$  decays to zero for every bounded initial datum  $\bar{\rho}$ ?
- (d) If the answer to Question (c) is positive, does it exist a velocity field, bounded in  $W^{1,p}$  uniformly in time, such that for any initial data  $\bar{\rho}$  the decay to zero of  $\text{mix}(\rho(t, \cdot))$  is precisely exponential?

We observed in Remark 1.4(iii) that our construction provides an example of palenstrophy-constrained flow such that  $\text{mix}(\rho(t, \cdot))$  decays polynomially in time. More in general, the self-similarity ansatz implies polynomial decay of  $\text{mix}(\rho(t, \cdot))$  in the case the velocity field is bounded in  $W^{s,p}$  uniformly in time for some  $s > 1$ . However, the numerical results mentioned in §1.5(d) support an exponential decay also for  $s > 1$ . If this were the case, we would deduce that for  $s > 1$  self-similarity is too strong a constraint, which only allows for sub-optimal decay rates (polynomial vs. exponential). This result would be in stark contrast with the case  $s = 1$ , for which the optimal decay rate can be obtained within self-similar evolutions. We therefore point out the following important question:

- (e) Does it exist a bounded initial datum  $\bar{\rho}$  and a velocity field bounded in  $W^{s,p}$  uniformly in time for some  $s > 1$  such that  $\text{mix}(\rho(t, \cdot))$  decays exponentially in time?

Such an example has necessarily to be non self-similar. The analysis in [17] implies in addition that such an example cannot be realized with a “localized” flow: roughly speaking, once the solution has been mixed to a certain scale, it can be more convenient to “unmix” it before reaching a lower mixing scale.

As mentioned in §1.5, examples of enstrophy-constrained flows that saturate the exponential decay rate (1.2) have been constructed in [41]. There, the authors utilize a cellular flow consisting of pseudo-rotations on a family of nested tilings of the square, and are able to obtain exponential mixing of every bounded initial datum by means of a velocity field bounded in  $W^{1,p}$  uniformly in time in the range  $1 \leq p \leq \bar{p}$  for some  $\bar{p} > 2$ . Therefore, this construction provides a partial answer to Question (b) above. Their nice geometric argument is based on a “stopping time” for the pseudo-rotation, which is determined by a clever application of the intermediate value theorem for continuous functions. Their construction also applies in the range  $\bar{p} < p < \infty$ , giving a mixing rate which is slightly slower than exponential, thus answering Question (a) above.

In comparison with [41], our construction apply only to specific choices of initial data. On the other hand, we obtain exponential mixing of the solution in the full range  $1 \leq p \leq \infty$ , even in the Lipschitz case. Moreover, our strategy has a clear geometric flavor, and generates velocity fields and solutions which are smooth. This last fact is relevant for the full scaling analysis (recall Remark 1.4(iii)) and for the application to the study of the loss of regularity for continuity equations, which will be fully addressed in a forthcoming paper (see §1.9 for a brief discussion). In addition, our examples provide an important insight into the geometrical properties of regular Lagrangian flows (see §1.8).

**1.8. Geometry of regular Lagrangian flows.** An important aspect of our work concerns properties of solutions to the Cauchy problem for the continuity equation (1.1) and of the associated regular Lagrangian flows.<sup>8</sup> In detail, the construction in Section 5 (see Remark 5.1) gives an example of a velocity field in two space dimensions that belongs to the space  $W^{s,p}$  for every  $s, p$  such that  $W^{s,p}$  does not embed in the Lipschitz class, i.e., for  $s < 2/p + 1$ , with the following properties:

- The associated regular Lagrangian flow does not preserve the connectedness of sets;

---

<sup>8</sup> That of regular Lagrangian flows is the appropriate notion for the flow generated by an ordinary differential equation (ODE for short) for which the velocity field has low regularity. A regular Lagrangian flow in  $\mathbb{R}^d$  solves the ODE for almost every initial point, and additionally preserves the  $d$ -dimensional Lebesgue measure up to a bounded factor. The theory in [20, 5] guarantees that, if the velocity field is Sobolev or  $BV$  and has bounded divergence, then there exists a unique regular Lagrangian flow associated to it.

- The set of initial points for which the ODE that generates the flow has more than one solution contains a full segment;
- Such a segment is “compressed” by the regular Lagrangian flow to a single point.<sup>9</sup>

Moreover, a time-reparametrization of our example in Section 8 gives an example of a bounded, compactly supported, divergence-free velocity field  $u$  such that  $u(t, \cdot) \in \text{Lip}(\mathbb{R}^2)$  for almost every  $0 \leq t \leq 1$ , and for which there is no uniqueness of solutions for the associated continuity equation. Indeed, such a velocity field fails to belong to  $L^1([0, 1]; \text{Lip}(\mathbb{R}^2))$ : the Lip norm blows up as  $t \downarrow 0$ . This example improves on the result in [18] in the  $BV$  case.

**1.9. Follow up: loss of regularity for continuity equations.** Mixing by shearing and filamentation increases positive Sobolev norms of the solution  $\rho$ , saturating the exponential growth which follows from the classical Grönwall inequality. Analytically, this can be seen by “dualizing” the exponential decay of the negative Sobolev norms in (1.3).

In a forthcoming paper [3], we will present an example of a velocity field in  $W^{1,p}$  for any  $1 \leq p < \infty$  that is regular except at a point and a smooth  $\bar{\rho}$  such that for  $t > 0$  the corresponding solution of (1.1) leaves instantly any Sobolev space  $H^s$  with  $s > 0$ . Extensions to Sobolev regularity of order higher than 1 are also possible.

Lack of propagation of the continuity and of the  $BV$  regularity for the continuity equation was already observed in [14]. More recently, lack of Sobolev regularity of order one for the flow of  $W^{1,p}$  velocity fields was also observed in [26], using a different construction that exploits a randomization procedure on certain basic elements of the flow.

**Acknowledgements.** This work was started during a visit of the first and third authors at the University of Basel. Their stay has been partially supported by the Swiss National Science Foundation grants 140232 and 156112. The visits of the second author to Pisa have been supported by the University of Pisa PRA project “Metodi variazionali per problemi geometrici [Variational Methods for Geometric Problems]”. The third author was partially supported by the US National Science Foundation grants DMS 1009713, 1009714, and 1312727.

## 2. PRELIMINARIES

Throughout the whole paper we will make extensive use of homogeneous Sobolev spaces with real (differentiation) order and of their properties. We present here their definition and the main properties of interest for our work, namely those regarding scaling, interpolation, and embeddings. For a systematic exposition we

<sup>9</sup> By definition, a regular Lagrangian flow in  $\mathbb{R}^d$  does not compress  $d$ -dimensional sets to null set. We see here that it can compress 1-dimensional sets to 0-dimensional sets.

refer the reader to [10, 8, 19, 24, 40]. In the last part of the section we define the two notions of mixing scale that we will use in all our work.

We limit our presentation to the two-dimensional case, however all definitions and results can be extended with obvious changes to the case of higher space dimensions. We work both on the full plane  $\mathbb{R}^2$  and on the two-dimensional torus, which we denote by  $\mathbb{T}^2 := \mathbb{R}^2/\mathbb{Z}^2$ . The Fourier transform of a tempered distribution  $f \in \mathcal{S}'(\mathbb{R}^2)$  is denoted by  $\hat{f}$  or by  $\mathcal{F}(f)$ , while the inverse Fourier transform of  $g$  is denoted by  $\mathcal{F}^{-1}(g)$ . Given a distribution  $f \in \mathcal{D}'(\mathbb{T}^2)$ , for  $k \in \mathbb{Z}^2$  we denote by  $\hat{f}(k)$  its  $k$ -th Fourier coefficient.

**2.1. Homogeneous Sobolev spaces  $\dot{H}^s$ .** For  $s \in \mathbb{R}$ , we say that a distribution  $f \in \mathcal{D}'(\mathbb{T}^2)$  on the torus belongs to the homogeneous Sobolev space  $\dot{H}^s(\mathbb{T}^2)$  if

$$\|f\|_{\dot{H}^s(\mathbb{T}^2)}^2 := \sum_{k \in \mathbb{Z}^2} |k|^{2s} |\hat{f}(k)|^2 < \infty. \quad (2.1)$$

If  $f \in \mathcal{S}'(\mathbb{R}^2)$  is a tempered distribution on the plane, we say that  $f$  belongs to the homogeneous Sobolev space  $\dot{H}^s(\mathbb{R}^2)$  if  $\hat{f} \in L^1_{\text{loc}}(\mathbb{R}^2)$  and

$$\|f\|_{\dot{H}^s(\mathbb{R}^2)}^2 := \int_{\mathbb{R}^2} |\xi|^{2s} |\hat{f}(\xi)|^2 d\xi < \infty. \quad (2.2)$$

We remark that homogeneous Sobolev spaces do not form a scale, due to the singularity of the multiplier at the origin in frequency space. In particular, it is generally not true that any square integrable function is automatically in  $\dot{H}^s$ , for  $s < 0$ .

*Remark 2.2.* (i) From (2.1) we immediately recognize that, in order for a function  $f \in L^1(\mathbb{T}^2)$  to belong to some  $\dot{H}^s(\mathbb{T}^2)$  with  $s < 0$ , it is necessary that  $\hat{f}(0) = 0$ . This corresponds to the zero average<sup>10</sup> condition  $\int_{\mathbb{T}^2} f = 0$ . Conversely, let  $f \in L^1(\mathbb{T}^2)$  be a function with zero average. Since the sequence of its Fourier coefficients  $\{\hat{f}(k)\}_{k \in \mathbb{Z}^2}$  is bounded, we deduce that such a function necessarily belongs to  $\dot{H}^{-s}(\mathbb{T}^2)$  for every  $s < -\frac{1}{2}$ .

(ii) Analogously, given a function  $f \in L^1(\mathbb{R}^2)$ , its Fourier transform  $\hat{f}$  is continuous. If  $s \leq -1$  the singularity at  $\xi = 0$  in (2.2) is not integrable, unless  $\hat{f}(0) = 0$ , which again corresponds to the zero average condition  $\int_{\mathbb{R}^2} f = 0$ .

(iii) In the case when  $f \in L^1(\mathbb{R}^2)$  has compact support something more can be said. In this case, Paley-Wiener theorem implies that the Fourier transform  $\hat{f}$  is an analytic function. In particular, there is a constant  $C > 0$  for which  $|\hat{f}(\xi) - \hat{f}(0)| \leq C|\xi|$  for any  $|\xi| \leq 1$ . If  $f$  additionally has zero average, we deduce that the singularity at  $\xi = 0$  in (2.2) is integrable for every  $s > -2$ .

(iv) Let  $f \in L^2(\mathbb{R}^2)$  have compact support and zero average. Since  $\hat{f} \in L^\infty(\mathbb{R}^2)$ , using item (iii) above we find that  $f \in \dot{H}^s(\mathbb{R}^2)$  for any  $-2 < s < -1$ . Combining

<sup>10</sup> Recalling that the functional mixing scale associated to a solution of (1.1) is given by its norm in  $\dot{H}^{-1}$ , we chose to work with zero-average solutions in §1.1 (also recall Footnote 1).

this fact with the assumption  $f \in L^2(\mathbb{R}^2)$ , the interpolation property (2.10) below gives that  $f \in \dot{H}^s(\mathbb{R}^2)$  for any  $-2 < s \leq 0$ .

**2.3. Homogeneous Sobolev spaces  $\dot{W}^{s,p}$ .** In the particular case  $s \geq 0$  we extend the definition in §2.1 to an arbitrary summability exponent  $1 < p < \infty$ .<sup>11</sup> We say that a distribution  $f \in \mathcal{D}'(\mathbb{T}^2)$  on the torus belongs to the homogeneous Sobolev space  $\dot{W}^{s,p}(\mathbb{T}^2)$  if

$$\sum_{k \in \mathbb{Z}^2} |k|^s \hat{f}(k) e^{ikx} \in L^p(\mathbb{T}^2), \quad (2.3)$$

and we let  $\|f\|_{\dot{W}^{s,p}(\mathbb{T}^2)}$  be the  $L^p(\mathbb{T}^2)$  norm of the function in (2.3). In general, elements of  $\dot{W}^{s,p}(\mathbb{T}^2)$  are equivalence classes modulo constants.

If  $f \in \mathcal{S}'(\mathbb{R}^2)$  is a tempered distribution on the plane, we say that  $f$  belongs to the homogeneous Sobolev space  $\dot{W}^{s,p}(\mathbb{R}^2)$  if  $\hat{f} \in L^1_{\text{loc}}(\mathbb{R}^2)$  and

$$\mathcal{F}^{-1}(|\xi|^s \hat{f}(\xi)) \in L^p(\mathbb{R}^2), \quad (2.4)$$

and we let  $\|f\|_{\dot{W}^{s,p}(\mathbb{R}^2)}$  be the  $L^p(\mathbb{R}^2)$  norm of the function in (2.4). The condition that  $\hat{f} \in L^1_{\text{loc}}(\mathbb{R}^2)$  guarantees that this quantity is a norm. In general, the spaces  $\dot{W}^{s,p}(\mathbb{R}^2)$  are spaces of equivalence classes of distributions modulo polynomials.

In our work, homogeneous spaces will be used only to measure the “size” of given functions and velocity fields, which will be typically be regular. In particular, the issue of completeness (which holds only for specific values of  $s$  given our definition) and seminorms will not arise.

*Remark 2.4.* (i) The non-homogeneous Sobolev spaces  $H^s$  and  $W^{s,p}$  are defined by replacing in (2.1), (2.2), (2.3), and (2.4) the symbols  $|k|$  and  $|\xi|$  by the symbols  $\langle k \rangle := \sqrt{1 + |k|^2}$  and  $\langle \xi \rangle := \sqrt{1 + |\xi|^2}$  respectively. The norms are equivalent on the torus for functions with zero average.

(ii) It is possible to prove that, if  $s = m \in \mathbb{N}$ , then  $\dot{W}^{m,p}(\mathbb{R}^2) \cap L^p(\mathbb{R}^2)$  coincides with the usual Sobolev space  $W^{m,p}(\mathbb{R}^2)$  consisting of those  $L^p(\mathbb{R}^2)$  functions possessing weak derivatives of order less or equal than  $m$  in  $L^p(\mathbb{R}^2)$ . This however does not hold in the borderline cases  $p = 1$  and  $p = \infty$ .

(iii) In contrast to the case of negative spaces (see Remark 2.2(i)-(ii)), it is not necessary for functions to have zero average to belong to  $\dot{W}^{s,p}$  with  $s \geq 0$ . Since we will measure the regularity of the velocity fields in terms of  $\dot{W}^{s,p}$  norms with  $s \geq 0$ , we will not need to prescribe conditions about the average of the velocity fields. In addition, none of the velocity fields in this work will be spatially constant, and hence we can assume that (2.3) defines a norm. Moreover, in the case of the plane  $\mathbb{R}^2$ , we will deal with velocity fields that are bounded and compactly supported, therefore the local integrability of the Fourier transform will be guaranteed.

<sup>11</sup> Only the spaces  $\dot{W}^{s,p}$  with  $s \geq 0$  will be needed for our scopes (see [24, 40] for a discussion of homogeneous spaces with regularity index  $s \in \mathbb{R}$ ).

**2.5. Lipschitz-Hölder spaces.** For notational convenience, in this paper we denote by  $\dot{W}^{s,\infty}(\mathbb{T}^2)$ , resp.  $\dot{W}^{s,\infty}(\mathbb{R}^2)$ , the homogeneous Lipschitz-Hölder space on  $\mathbb{T}^2$ , resp. on  $\mathbb{R}^2$ , defined as follows. Since the definition of these spaces on  $\mathbb{T}^2$  and on  $\mathbb{R}^2$  is the same, below we do not write explicitly the domain.

If  $s = k \in \mathbb{N}$  is greater or equal to 1, we say that  $f \in \dot{W}^{k,\infty}$  if  $f \in C^{k-1}$  and there is a constant  $C > 0$  such that

$$|f^{(k-1)}(x) - f^{(k-1)}(y)| \leq C|x - y| \quad \text{for every } x \text{ and } y. \quad (2.5)$$

We let  $\|f\|_{\dot{W}^{k,\infty}}$  be the minimal constant  $C$  for which (2.5) holds.

If  $s$  is not an integer, we let  $\lfloor s \rfloor$  be the largest integer smaller than  $s$ . In this case, we say that  $f \in \dot{W}^{s,\infty}$  if  $f \in C^{\lfloor s \rfloor}$  and there is a constant  $C > 0$  such that

$$|f^{(\lfloor s \rfloor)}(x) - f^{(\lfloor s \rfloor)}(y)| \leq C|x - y|^{s - \lfloor s \rfloor} \quad \text{for every } x \text{ and } y. \quad (2.6)$$

We let  $\|f\|_{\dot{W}^{s,\infty}}$  be the minimal constant  $C$  for which (2.6) holds.

*Remark 2.6.* In two space dimensions, the Sobolev space  $\dot{W}^{s,p}$  embeds in the Lipschitz space  $\dot{W}^{1,\infty}$  if  $s > 1$  and  $p > \frac{2}{s-1}$ .

**2.7. Scaling properties.** We will be frequently interested in the behavior of homogeneous Sobolev norms under rescaling of a given function  $f$ . Given  $\lambda > 0$ , we set

$$f_\lambda(x) := f\left(\frac{x}{\lambda}\right). \quad (2.7)$$

If  $f$  is defined on the torus and  $1/\lambda$  is an integer, then the function  $f_\lambda$  in (2.7) is well defined on the torus and it holds

$$\|f_\lambda\|_{\dot{W}^{s,p}(\mathbb{T}^2)} = \lambda^{-s} \|f\|_{\dot{W}^{s,p}(\mathbb{T}^2)}. \quad (2.8)$$

If  $f$  is defined on the plane, then the function  $f_\lambda$  in (2.7) is well defined for any  $\lambda > 0$  and it holds

$$\|f_\lambda\|_{\dot{W}^{s,p}(\mathbb{R}^2)} = \lambda^{\frac{2}{p}-s} \|f\|_{\dot{W}^{s,p}(\mathbb{R}^2)}. \quad (2.9)$$

When  $p = 2$ , both formulas (2.8) and (2.9) hold for  $s \in \mathbb{R}$  (with norms in  $\dot{H}^s$ ).

*Remark 2.8.* The difference between the exponents in formulas (2.8) and (2.9) is due to the fact that the rescalings on the torus and on the plane are two different operations. The rescaling of a single bump on the plane remains a single bump, while on the torus  $1/\lambda^2$  rescaled copies are produced.

**2.9. Interpolation.** We will frequently rely on the following standard interpolation inequality. If  $s_1 < s < s_2$  and  $s = \vartheta s_1 + (1 - \vartheta)s_2$ , then

$$\|f\|_{\dot{H}^s} \leq \|f\|_{\dot{H}^{s_1}}^\vartheta \|f\|_{\dot{H}^{s_2}}^{1-\vartheta} \quad (2.10)$$

and

$$\|f\|_{\dot{W}^{s,p}} \leq \|f\|_{\dot{W}^{s_1,p}}^\vartheta \|f\|_{\dot{W}^{s_2,p}}^{1-\vartheta}, \quad (2.11)$$

where both inequalities hold both with domain  $\mathbb{T}^2$  and  $\mathbb{R}^2$ . The same holds in the case  $p = \infty$  in the context of Lipschitz-Hölder spaces (recall §2.5) and can be proved with a simple direct argument.

We next introduce the two notions of mixing scale that will be employed in this paper to quantify the level of mixedness of the solution  $\rho$ . Both definitions can be given on the torus and on the plane.

The first notion is based on homogeneous Sobolev norms. From a physical point of view, the choice of the order  $-1$  is the most convenient, since the norm in  $\dot{H}^{-1}$  scales as a length. However, from a mathematical point of view, every negative homogeneous Sobolev norm would behave in a similar way.

**2.10. Definition. Functional mixing scale** [31, 36]. The functional mixing scale of  $\rho(t, \cdot)$  is  $\|\rho(t, \cdot)\|_{\dot{H}^{-1}(\mathbb{T}^2)}$ .

The second notion is more geometric and has been originally introduced in [13] for solutions with value  $\pm 1$ . We use the following generalization introduced in [41], which has the advantage of making sense for every bounded solution  $\rho$ , without any constraint on its values.

**2.11. Definition. Geometric mixing scale** [13]. Given  $0 < \kappa < 1$ , the geometric mixing scale of  $\rho(t, \cdot)$  is the infimum  $\varepsilon(t)$  of all  $\varepsilon > 0$  such that for every  $x \in \mathbb{T}^2$  there holds

$$\frac{1}{\|\rho(t, \cdot)\|_\infty} \left| \int_{B_\varepsilon(x)} \rho(t, y) dy \right| \leq \kappa. \quad (2.12)$$

The parameter  $\kappa$  is fixed and plays a minor role in the definition. Informally, in order for  $\rho(t, \cdot)$  to have geometric mixing scale  $\varepsilon(t)$ , we require that the average of the solution on every ball of radius  $\varepsilon(t)$  is essentially zero. In a certain sense, we require the property of having (approximately) zero average to be localizable to balls of radius  $\varepsilon(t)$ .

*Remark 2.12.* In [13] the following definition was given for solutions with value  $\pm 1$ . Given  $0 < \tilde{\kappa} < 1/2$ , (2.12) is replaced by the requirement that

$$\tilde{\kappa} \leq \frac{|\{\rho(t, \cdot) = 1\} \cap B_\varepsilon(x)|}{|B_\varepsilon(x)|} \leq 1 - \tilde{\kappa}. \quad (2.13)$$

Informally, according to [13], in order for  $\rho(t, \cdot)$  to have geometric mixing scale  $\varepsilon(t)$ , it is required that every ball of radius  $\varepsilon(t)$  contains a “substantial portion” of both level sets  $\{\rho(t, \cdot) = 1\}$  and  $\{\rho(t, \cdot) = -1\}$ . It is easily seen that the two definitions correspond if  $\kappa = 1 - 2\tilde{\kappa}$ .

As previously mentioned, the two notions of mixing scale are not equivalent, though they are strongly related (we refer to [34] for a further discussion on this point; see also Lemma 3.5).

### 3. SCALING ANALYSIS IN A SELF-SIMILAR CONSTRUCTION

A conceivable procedure for mixing consists of a self-similar evolution. Such a procedure, together with the related scaling analysis, has been presented in [4]. Let  $s \geq 0$  and  $1 \leq p \leq \infty$  be fixed and assume the following:

**3.1. Assumption. Self-similar base element.** There exist a velocity field  $u_0$  and a (not identically zero) solution  $\rho_0$  to (1.1), both defined for  $0 \leq t \leq 1$  and  $x \in \mathbb{T}^2$ , such that:

- (i)  $u_0$  is bounded in  $\dot{W}^{s,p}(\mathbb{T}^2)$  uniformly in time, bounded, and divergence-free;
- (ii)  $\rho_0$  is bounded and has zero average;
- (iii) there exists a positive constant  $\lambda$ , with  $1/\lambda$  an integer greater or equal than 2, such that

$$\rho_0(1, x) = \rho_0\left(0, \frac{x}{\lambda}\right).$$

An explicit example of a  $u_0$  and a  $\rho_0$  satisfying this assumption will be given in Section 5 for  $s = 1$  and every  $1 \leq p < \infty$ .

For later use, we give the following definitions:

**Definition 3.2.** (i) Given  $\lambda > 0$ , with  $1/\lambda$  an integer, we denote by  $\mathcal{T}_\lambda$  the tiling of  $\mathbb{T}^2$  with squares of sidelength  $\lambda$ , consisting of  $1/\lambda^2$  open squares in  $\mathbb{T}^2$  of the form

$$\{(x, y) \in \mathbb{T}^2 : k\lambda < x < (k+1)\lambda \text{ and } h\lambda < y < (h+1)\lambda\},$$

for  $k, h = 0, \dots, 1/\lambda - 1$ .

(ii) Denoting by  $\mathcal{Q}$  the unit open square  $(-1/2, 1/2)^2 \subset \mathbb{R}^2$  the tiling  $\mathcal{T}_\lambda$  of  $\mathcal{Q}$  is defined analogously. Given any square  $Q \in \mathcal{T}_{\lambda^n}$ , we denote by  $r_Q$  its center, so that  $Q = \lambda^n \mathcal{Q} + r_Q$ .

**3.3. A self-similar construction.** Fix a positive parameter  $\tau$  (that will be determined later). For each integer  $n = 1, 2, \dots$  and for  $t \in [0, \tau^n]$  we set

$$u_n(t, x) := \frac{\lambda^n}{\tau^n} u_0\left(\frac{t}{\tau^n}, \frac{x}{\lambda^n}\right), \quad \rho_n(t, x) := \rho_0\left(\frac{t}{\tau^n}, \frac{x}{\lambda^n}\right).$$

Notice that  $\rho_n$  is a solution of (1.1) corresponding to the velocity field  $u_n$ . Moreover, because of Assumption 3.1(iii),

$$\rho_n(\tau^n, x) = \rho_{n+1}(0, x). \tag{3.1}$$

Let us now define  $u$  and  $\rho$  by patching together the velocity fields  $u_0, u_1, \dots$  and the corresponding solutions  $\rho_0, \rho_1, \dots$ . In detail, we set

$$u(t, x) := u_n(t - T_n, x), \quad \rho(t, x) := \rho_n(t - T_n, x)$$

for  $T_n \leq t < T_{n+1}$ , and  $n = 1, 2, \dots$ , where

$$T_n := \sum_{i=0}^{n-1} \tau^i, \quad \text{for } n = 1, 2, \dots, \infty.$$

Notice that  $u$  and  $\rho$  are defined for  $0 \leq t < T_\infty$ . Moreover, recalling equation (3.1),  $\rho$  is a weak solution<sup>12</sup> of the Cauchy problem for (1.1) with velocity field  $u$  and initial condition  $\bar{\rho}(x) = \rho_0(0, x)$ .

<sup>12</sup> This can be easily seen by writing the weak formulation of the continuity equation (1.1) on each time interval  $[T_n, T_{n+1}]$  with test functions in  $C^\infty([T_n, T_{n+1}])$ .



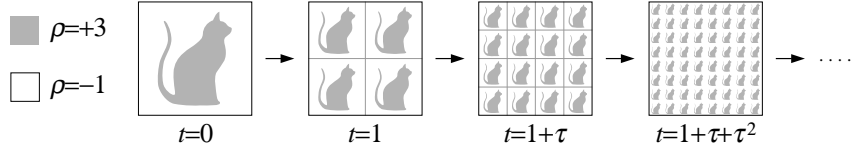


FIGURE 1. Example of self-similar evolution for a function  $\rho$  taking only two values.

Using (2.8) we can compute

$$\|u_n(t, \cdot)\|_{\dot{W}^{s,p}(\mathbb{T}^2)} = \left(\frac{\lambda^{1-s}}{\tau}\right)^n \left\|u_0\left(\frac{t}{\tau^n}, \cdot\right)\right\|_{\dot{W}^{s,p}(\mathbb{T}^2)}.$$

If we set  $\tau = \lambda^{1-s}$ , the formula above gives that  $u$  is bounded in  $\dot{W}^{s,p}(\mathbb{T}^2)$  uniformly in time. Moreover,

$$\|\rho_n(t, \cdot)\|_{\dot{H}^{-1}(\mathbb{T}^2)} = \lambda^n \left\|\rho_0\left(\frac{t}{\tau^n}, \cdot\right)\right\|_{\dot{H}^{-1}(\mathbb{T}^2)} \leq M\lambda^n,$$

where we have set

$$M := \sup_{0 \leq t \leq 1} \|\rho_0(t, \cdot)\|_{\dot{H}^{-1}(\mathbb{T}^2)}.$$

This can be rewritten as

$$\|\rho(t, \cdot)\|_{\dot{H}^{-1}(\mathbb{T}^2)} \leq M\lambda^n, \quad \text{for } T_n \leq t < T_{n+1}. \quad (3.2)$$

We can now consider the following three different scenarios:

- (1)  $s < 1$ , then  $\tau = \lambda^{1-s} < 1$ . In this case,  $T_\infty$  is finite and

$$\|\rho(t, \cdot)\|_{\dot{H}^{-1}(\mathbb{T}^2)} \rightarrow 0,$$

as  $t \rightarrow T_\infty$ . That is, we have perfect mixing in finite time;

- (2)  $s = 1$ , then  $\tau = 1$ . In this case,  $T_\infty = \infty$  and  $T_n = n$ , therefore the inequality  $t < T_{n+1}$  in (3.2) becomes  $t - 1 < n$ . Hence, the estimate in (3.2) yields the following exponential decay of the functional mixing scale:

$$\|\rho(t, \cdot)\|_{\dot{H}^{-1}(\mathbb{T}^2)} \leq M\lambda^{t-1};$$

- (3)  $s > 1$ , then  $\tau > 1$ . In this case,  $T_\infty = \infty$  and

$$T_n = \frac{\tau^n - 1}{\tau - 1} = \frac{\lambda^{(1-s)n} - 1}{\lambda^{1-s} - 1}.$$

By the same argument as above, (3.2) implies the following polynomial decay:

$$\|\rho(t, \cdot)\|_{\dot{H}^{-1}(\mathbb{T}^2)} \leq M \frac{[1 + t(\lambda^{1-s} - 1)]^{-\frac{1}{s-1}}}{\lambda} \simeq C(M, \lambda, s) t^{-\frac{1}{s-1}}.$$

What we have just discussed can be summarized in the following theorem:

**Theorem 3.4.** *Given  $s \geq 0$  and  $1 \leq p \leq \infty$ , under Assumption 3.1, there exist a bounded divergence-free velocity field  $u$  and a weak solution  $\rho$  of the Cauchy problem for (1.1), such that  $u$  is bounded in  $\dot{W}^{s,p}(\mathbb{T}^2)$  uniformly in time and the functional mixing scale of  $\rho$  exhibits the following behavior depending on  $s$ :*

- (1) *Case  $s < 1$ : perfect mixing in finite time;*
- (2) *Case  $s = 1$ : exponential decay;*
- (3) *Case  $s > 1$ : polynomial decay.*

In fact, all homogeneous negative Sobolev norms  $\|\rho(t)\|_{\dot{H}^{-r}}$  (with  $r > 0$ ) would exhibit the same behavior, with the only difference being in the constant for the exponential decay and the exponent for the polynomial decay, which depend on  $r$ . We observe that, in the case  $s > 1$ , such self-similar scaling analysis does not yield the known exponential lower bound for the (geometric and functional) mixing scale, which is supposed to be optimal; rather, it yields a slower polynomial decay in time.

The following lemma proves that the geometric mixing scale  $\varepsilon(t)$  exhibits the same behavior, detailed in Theorem 3.4, as the functional mixing scale.

**Lemma 3.5.** *Let  $\rho$  be a bounded function such that*

$$\oint_Q \rho \, dy = 0 \quad (3.3)$$

*for every square  $Q \in \mathcal{T}_{\lambda^n}$ . Then the geometric mixing scale of  $\rho$  as in (2.12) is less or equal than*

$$\frac{4\sqrt{2} \lambda^n}{\kappa}. \quad (3.4)$$

**Proof.** We fix an arbitrary ball  $B_\varepsilon(x)$ . Using (3.3) we can estimate

$$\begin{aligned} \frac{1}{\|\rho\|_\infty} \left| \int_{B_\varepsilon(x)} \rho \, dy \right| &\leq \frac{1}{\|\rho\|_\infty} \sum_{\substack{Q \in \mathcal{T}_{\lambda^n} \\ Q \cap \partial B_\varepsilon(x) \neq \emptyset}} \int_Q |\rho| \, dy \\ &\leq \frac{1}{\|\rho\|_\infty} \int_{B_{\varepsilon+\sqrt{2}\lambda^n}(x) \setminus B_{\varepsilon-\sqrt{2}\lambda^n}(x)} |\rho| \, dy \\ &\leq \pi [(\varepsilon + \sqrt{2}\lambda^n)^2 - (\varepsilon - \sqrt{2}\lambda^n)^2] = 4\sqrt{2}\pi\varepsilon\lambda^n, \end{aligned}$$

where the second inequality follows from elementary geometric considerations. Hence,

$$\frac{1}{\|\rho\|_\infty} \left| \int_{B_\varepsilon} \rho \, dx \right| \leq \frac{4\sqrt{2} \lambda^n}{\varepsilon},$$

and the right-hand side is less or equal than  $\kappa$  for every  $\varepsilon$  greater or equal than the quantity in (3.4). Therefore, from (2.12) the desired estimate on the geometric mixing scale follows.  $\square$

**3.6. Regularity in time.** Under Assumption 3.1, the self-similar construction described above ensures Sobolev regularity of the velocity field with respect to the space variable, uniformly in time. No regularity with respect to the time variable is provided.

In fact, in all examples presented in this paper, the velocity field is piecewise smooth with respect to both space and time variables. If the velocity field is smooth in time on two adjacent time intervals, and if it can be smoothly extended to the closure of each of them, then the discontinuity across the interface of the two intervals can be eliminated. Indeed, it is enough to replace in each interval  $u$  and  $\rho$  by

$$\tilde{u}(t, x) := \eta'(t) u(\eta(t), x), \quad \tilde{\rho}(t, x) := \rho(\eta(t), x),$$

where in each interval the smooth function  $\eta$  is chosen to be increasing, surjective, and constant in a small (left or right) neighborhood of each of endpoints of the interval. It is immediate to check that  $\tilde{\rho}$  solves the Cauchy problem for (1.1) with velocity field  $\tilde{u}$ , that  $\tilde{u}$  is smooth on the union of the closures of the two time intervals, and that the value of the solution at the endpoints of both intervals has not changed.

We remark that the argument above does not apply in case the velocity field lacks a smooth extension to the closure of (at least) one time interval. In such a case the time discontinuity cannot be eliminated. Our example in Section 5 indeed contains singularities, which is unavoidable, since topological properties of the transported sets are changed along the time evolution.

#### 4. FIRST GEOMETRIC CONSTRUCTION

In the main result of this section (Proposition 4.6) we show that given a regular set  $E$  in the plane which evolves smoothly in time, we can construct a smooth divergence-free velocity field  $u$  such that the characteristic function of  $E$  solves the continuity equation (1.1) associated to  $u$ . In the next section we use this result to produce the building blocks for the examples of optimal mixers given in this work.

We begin by introducing some notation. Given a vector  $v = (v_1, v_2) \in \mathbb{R}^2$ , we denote by  $v^\perp$  its rotation by  $90^\circ$  counter-clockwise, that is,

$$v^\perp := (-v_2, v_1).$$

Given a set  $E$  in  $\mathbb{R}^2$  and a point  $x \in \mathbb{R}^2$ , we denote by  $\text{dist}(x, E)$  the distance of  $x$  from  $E$ , defined in the standard way by

$$\text{dist}(x, E) := \inf \{|x - y| \mid y \in E\}.$$

If there exists exactly one point  $y \in E$  where such infimum is attained, this point will be called the *projection* of  $x$  onto  $E$  and denoted by  $p_E(x)$ . For every  $r > 0$ , we shall also denote by  $B(E, r)$  the open  $r$ -neighbourhood of  $E$ , that is,

$$B(E, r) := \{x \in \mathbb{R}^2 : \text{dist}(x, E) < r\}.$$

**4.1. Paths and curves.** In this paper we consider only two kinds of paths.

A *closed path* is a continuous map  $\gamma = \gamma(s)$  from the circle, which we identify with the one-dimensional torus  $\mathbb{T}^1 := \mathbb{R}/\mathbb{Z}$ , to the plane  $\mathbb{R}^2$ . Moreover we require that  $\gamma$  is injective, of class  $C^1$ , and satisfies  $\dot{\gamma}(s) \neq 0$  for all  $s \in \mathbb{T}^1$ . A *closed (oriented) curve* is the image  $\Gamma = \gamma(\mathbb{T}^1)$  of a closed path  $\gamma$ .

A *proper path* is a continuous map  $\gamma = \gamma(s)$  from the real line  $\mathbb{R}$  to the plane  $\mathbb{R}^2$  which is proper, that is,  $|\gamma(s)|$  tends to  $+\infty$  as  $s \rightarrow \pm\infty$ . As before, we require that  $\gamma$  is injective, of class  $C^1$ , and satisfies  $\dot{\gamma}(s) \neq 0$  for all  $s \in \mathbb{R}$ . A *proper (oriented) curve* is the image  $\Gamma = \gamma(\mathbb{R})$  of a proper path  $\gamma$ .

When we do not want to distinguish between closed and proper paths (or curves), we simply write path (or curve), and denote the parametrization domain, which is either  $\mathbb{T}^1$  or  $\mathbb{R}$ , by the letter  $J$ . As usual, the regularity of a curve  $\Gamma$  refers to the regularity of the parametrization  $\gamma$ .

Let  $\Gamma$  be a curve parametrized by  $\gamma$ . A *sub-arc* of  $\Gamma$  is any set of the form  $\gamma(J')$  where  $J'$  is an interval contained in  $J$ ; a sub-arc is *proper* if it is strictly contained in  $\Gamma$ .

The unit tangent vector  $\tau(x)$  and the unit normal vector  $\eta(x)$  at a point  $x = \gamma(s)$  in  $\Gamma$  are given by

$$\tau := \dot{\gamma}/|\dot{\gamma}|, \quad \eta := -\tau^\perp = -\dot{\gamma}^\perp/|\dot{\gamma}|.$$

In particular if  $|\dot{\gamma}|(s)$  is equal to the constant  $\ell$  for all  $s$  then  $\tau := \dot{\gamma}/\ell$ ,  $\eta := \dot{\gamma}^\perp/\ell$ , and the curvature  $\kappa(x)$  of  $\Gamma$  at the point  $x = \gamma(s)$  satisfies the equation

$$\kappa \eta = \ddot{\gamma}/\ell^2.$$

The *tubular radius* of  $\Gamma$  is the largest  $r \geq 0$  such that the map  $\Psi$  given by<sup>13</sup>

$$\Psi : (s, y) \mapsto \gamma(s) + y\eta(s) \tag{4.1}$$

is injective on  $J \times (-r, r)$ .

If  $\Gamma$  is of class  $C^2$  then the tubular radius is smaller than the *curvature radius*  $1/\kappa(x)$  for every  $x \in \Gamma$ .

If  $\Gamma$  is of class  $C^k$  with  $k \geq 2$  and the tubular radius  $r$  is strictly positive, the map  $\Psi$  is a diffeomorphism of class  $C^{k-1}$  from  $J \times (-r, r)$  to the tubular neighbourhood  $B(\Gamma, r)$ ; the projection  $p_\Gamma(x)$  is well-defined for every point  $x = \Psi(s, y)$  in  $B(\Gamma, r)$ , and agrees with  $\gamma(s)$ .

If  $\Gamma$  is closed and of class  $C^2$  then the tubular radius is strictly positive.

**4.2. Time-dependent paths and curves.** In this paper we often consider paths and curves which vary in time; in this case,  $\gamma$  is a map from the rectangle  $I \times J$  to the plane  $\mathbb{R}^2$ , where  $I$  is a time interval (open, closed, or else), and  $\Gamma$  is a map that to every  $t \in I$  associate a curve  $\Gamma(t)$  in  $\mathbb{R}^2$ ; when we speak of regularity for such objects we refer to the regularity of the parametrization map  $\gamma$  in both variables.

<sup>13</sup> With a slight abuse of notation, we sometimes write the geometric quantities  $\tau$ ,  $\eta$  and  $\kappa$  as functions of the parametrization variable  $s$  instead of  $x$ .

In the following we reserve the letter  $t$  for the time variable in  $I$  and the letter  $s$  for the parametrization variable in  $J$ , we write  $\dot{\gamma}$  for the partial derivative w.r.t.  $s$ , and  $\partial_t \gamma$  for the partial derivative w.r.t.  $t$ .

The *normal velocity*  $v_n = v_n(t, x)$  of  $\Gamma$  at time  $t$  and point  $x = \gamma(t, s)$  is the normal component of the vector  $\partial_t \gamma(t, s)$ , that is,

$$v_n := \partial_t \gamma \cdot \eta.$$

Note that the normal velocity does not change under reparametrization of  $\gamma$  in the variable  $s$ .

**4.3. Time-dependent domains.** A time-dependent domain is a map  $E$  that to every  $t$  in the time interval  $I$  associates an open subset  $E(t)$  of  $\mathbb{R}^2$ . We say that  $E$  is of class  $C^k$  if there exist finitely many time-dependent curves  $\Gamma_i$ , parametrized by paths  $\gamma_i : I \times J_i \rightarrow \mathbb{R}^2$  of class  $C^k$ , such that for every  $t \in I$  the boundary  $\partial E(t)$  can be written as disjoint union of the curves  $\Gamma_i(t)$ .

We also require that each parametrization is *counter-clockwise*, which means that the normal vector  $\eta$  defined in §4.1 agrees with the *inner normal* to the boundary  $\partial E$  at every time  $t$  and at every point  $x = \gamma_i(t, s)$ . Thus the normal velocity  $v_n$  defined in §4.2 agrees with the *outer normal velocity* of  $\partial E$ .

**4.4. Compatible velocity fields.** Let  $u$  be a continuous, time-dependent velocity field on  $\mathbb{R}^2$ . We say that  $u$  is *compatible* with a time-dependent curve  $\Gamma$  if, for every time  $t$  and every point  $x \in \Gamma(t)$ , the normal velocity  $v_n$  of  $\Gamma$  agrees with the normal component of  $u$ , that is

$$v_n = u \cdot \eta. \quad (4.2)$$

Accordingly, we say that  $u$  is *compatible* with a time-dependent domain  $E$  of class  $C^1$  if the normal component of  $u$  agrees with the outer normal velocity  $v_n$  of  $E$  at every time  $t$  and at every point  $x \in \partial E(t)$ .

Fix  $t_0 \in I$ , and let  $\{\Phi(t, \cdot) : t \in I\}$  be the flow (if it exists) associated to  $u$  with initial time  $t_0$ , which means that each  $\Phi(t, \cdot)$  is an homeomorphism from  $\mathbb{R}^2$  into  $\mathbb{R}^2$ , and that for every  $x_0 \in \mathbb{R}^2$  the map  $t \mapsto \Phi(t, x_0)$  solves the ordinary differential equation  $\dot{x} = u(t, x)$  with initial condition  $x(t_0) = x_0$ . Then the compatibility of  $u$  and  $\Gamma$  means that  $\Gamma(t) = \Phi(t, \Gamma(t_0))$  for every  $t \in I$ ; in particular the compatibility of  $u$  and  $E$  means that  $\partial E(t) = \Phi(t, \partial E(t_0))$ , which yields

$$E(t) = \Phi(t, E(t_0)) \quad \text{for every } t \in I.$$

Finally, it is well-known that the last identity implies that the characteristic function  $\rho(t, x) := 1_{E(t)}(x)$  is a distributional solution of the transport equation

$$\rho_t + u \cdot \nabla \rho = 0. \quad (4.3)$$

*Remark 4.5.* When  $u$  is divergence-free equation (4.3) agrees with the continuity equation (1.1) and therefore the velocity field  $u$  is compatible with the time-dependent domain  $E$  if and only if the characteristic function  $\rho(t, x) := 1_{E(t)}(x)$  is a distributional solution of (1.1).

Note that the latter condition makes sense also if  $u$  and  $E$  are not regular (we just need that  $u$  is locally in the class  $L^1$ , and that  $E$  is a measurable subset of  $I \times \mathbb{R}^2$ ) and therefore can be taken as a weak notion of compatibility.

In the rest of this section we address the following question: given a time-dependent curve  $\Gamma$ , or a time-dependent domain  $E$ , under which assumptions there exists a compatible velocity field  $u$  which is divergence-free?

We begin with a basic statement, which we then specialize according to our specific needs.

**Proposition 4.6.** *Let  $\Gamma$  be a time-dependent curve in  $\mathbb{R}^2$  with time interval  $I$  and of class  $C^k$  with  $k \geq 2$ , and let  $\bar{r} : I \rightarrow (0, +\infty)$  be a continuous function. Assume that for every  $t \in I$  the normal velocity  $v_n(t, \cdot)$  has compact support,<sup>14</sup> and satisfies*

$$\int_{\Gamma(t)} v_n(t, x) d\sigma(x) = 0. \quad (4.4)$$

*Then there exists a divergence-free velocity field  $u : I \times \mathbb{R}^2 \rightarrow \mathbb{R}^2$  of class  $C^{k-2}$  which is compatible with  $\Gamma$ , and such that the support of  $u(t, \cdot)$  is contained in  $B(\Gamma(t), \bar{r}(t))$  for every  $t \in I$ .*

*Moreover, under the additional assumption that for every  $t \in I$  the support of  $v_n(t, \cdot)$  is contained in a compact, proper sub-arc  $G(t)$  of  $\Gamma(t)$  which depends continuously in  $t$ ,<sup>15</sup> we can choose  $u$  so that the support of  $u(t, \cdot)$  is contained in  $B(G(t), \bar{r}(t))$  for every  $t \in I$ .*

*Remark 4.7.* (i) If  $\Gamma$  is closed, assumption (4.4) is necessary, in the sense that it is satisfied by every time-dependent closed path  $\Gamma$  which is compatible with a divergence-free velocity field  $u$ . Fix indeed  $t \in I$ , let  $E(t)$  be the bounded open set with boundary  $\Gamma(t)$ , and denote by  $\eta_{E(t)}$  the outer normal to  $\partial E(t)$ ; then the divergence theorem yields

$$\int_{\Gamma(t)} v_n d\sigma = \pm \int_{\partial E(t)} u \cdot \eta_{E(t)} d\sigma = \pm \int_{E(t)} \operatorname{div} u dx = 0,$$

where the sign  $\pm$  depends on whether the normal to  $\Gamma(t)$  agrees with  $\eta_{E(t)}$  or  $-\eta_{E(t)}$ .

(ii) A modification of the previous argument shows that assumption (4.4) is necessary if  $\Gamma$  is proper, and both  $v_n$  and  $u$  have compact support. However, if we do not require that  $u$  has compact support, then we can drop both the assumption that  $v_n$  has compact support and (4.4).

(iii) If  $\Gamma$  is a closed curve and agrees with the boundary of a bounded, time-dependent domain  $E$ , then it is well-known that

$$\int_{\Gamma(t)} v_n d\sigma = \frac{d}{dt} |E(t)| \quad \text{for every } t \in I.$$

<sup>14</sup> This requirement is clearly redundant when  $\Gamma$  is closed.

<sup>15</sup> The class of compact sub-arcs of  $\Gamma$  is endowed with the Hausdorff distance.

Therefore assumption (4.4) is equivalent to require that the area of  $E(t)$  is constant in  $t$ .

(iv) Proposition 4.6 can be generalized to higher dimensions, for instance to time-dependent surfaces with codimension one in  $\mathbb{R}^n$ , but such extensions require quite different proofs.

We consider now the special case of a curve which evolves homothetically in time. We first give a definition and a few remarks.

**4.8. Homothetic curves.** We say that a time-dependent curve  $\Gamma$  on the time interval  $I$  is homothetic in time if it can be represented as

$$\Gamma(t) = \lambda(t) \bar{\Gamma} = \{\lambda(t) x : x \in \bar{\Gamma}\} \quad (4.5)$$

for some curve  $\bar{\Gamma}$  and some function  $\lambda : I \rightarrow (0, +\infty)$ .

Let  $\bar{\gamma} : J \rightarrow \mathbb{R}^2$  be a path that parametrizes  $\bar{\Gamma}$ . Then the time-dependent path  $\gamma : I \times J \rightarrow \mathbb{R}^2$  given by

$$\gamma(t, s) := \lambda(t) \bar{\gamma}(s) \quad (4.6)$$

is a parametrization of  $\Gamma$ ; thus  $\Gamma$  is of class  $C^k$  when  $\bar{\Gamma}$  and  $\lambda$  are of class  $C^k$ .

Let  $\bar{\eta}$  be the normal to  $\bar{\Gamma}$  and let  $\bar{v} : \bar{\Gamma} \rightarrow \mathbb{R}$  be the function defined by

$$\bar{v}(x) := x \cdot \bar{\eta}(x). \quad (4.7)$$

Then a simple computation starting from (4.6) yields that the normal vector and the normal velocity of  $\Gamma$  (at  $t \in I$  and  $x \in \Gamma(t)$ ) are given by

$$\eta(t, x) = \bar{\eta}(x/\lambda(t)), \quad v_n(t, x) = \lambda'(t) \bar{v}(x/\lambda(t)). \quad (4.8)$$

Finally, let  $\bar{u}$  be an autonomous velocity field on  $\mathbb{R}^2$  such that

$$\bar{u}(x) \cdot \bar{\eta}(x) = \bar{v}(x) \quad (4.9)$$

for every  $x \in \bar{\Gamma}$ . Then using (4.8) one readily checks that the time-dependent velocity field  $u : I \times \mathbb{R}^2 \rightarrow \mathbb{R}^2$  defined by

$$u(t, x) := \lambda'(t) \bar{u}(x/\lambda(t)) \quad (4.10)$$

is compatible with the time-dependent curve  $\Gamma$ .

The next result specializes the statement of Proposition 4.6 to the case of homothetic curves.

**Proposition 4.9.** *Let be given a function  $\lambda : I \rightarrow (0, +\infty)$  and a proper curve  $\bar{\Gamma}$ , both of class  $C^k$  with  $k \geq 2$ , a positive number  $\bar{r}$  and a compact sub-arc  $\bar{G}$  of  $\bar{\Gamma}$  which contains the support of the function  $\bar{v}$  defined in (4.7). Assume moreover that*

$$\int_{\bar{\Gamma}} \bar{v} d\sigma = 0. \quad (4.11)$$

*Then the following statements hold:*

- (i) *there exists an autonomous velocity field  $\bar{u}$  on  $\mathbb{R}^2$  of class  $C^{k-2}$  which satisfies (4.9), is divergence-free, and its support is contained in  $B(\bar{G}, \bar{r})$ ;*

- (ii) if  $\Gamma$  is the time-dependent (homothetic) curve defined in (4.5) and  $u$  is the time-dependent velocity field defined in (4.10), then  $u$  is of class  $C^{k-2}$ , divergence-free and compatible with  $\Gamma$ , and the support of  $u(t, \cdot)$  is contained in  $B(\lambda(t)\bar{G}, \lambda(t)\bar{r})$  for every  $t \in I$ .

*Remark 4.10.* (i) The formula for the normal velocity in (4.8) shows that assumption (4.11) in Proposition 4.9 plays the role of assumption (4.4) in Proposition 4.6.

(ii) Proposition 4.9 does not apply to closed curves, because condition (4.11) is not verified if  $\bar{\Gamma}$  is closed. Let indeed  $E$  be a bounded open set with boundary  $\bar{\Gamma}$ ; then the divergence theorem yields

$$\int_{\bar{\Gamma}} \bar{v} d\sigma = \int_{\partial E} x \cdot \bar{\eta}(x) d\sigma(x) = \pm \int_E \operatorname{div}(x) dx = \pm 2|E| \neq 0,$$

where the sign  $\pm$  depends on whether  $\bar{\eta}$  is the inner or the outer normal of  $E$ .

(iii) It is easy to check that if the curve  $\bar{\Gamma}$  agrees outside some open ball  $B = B(0, r)$  with two half-lines  $L_-, L_+$  starting from the origin, then the function  $\bar{v}$  has compact support (and the converse is also true).

If, in addition,  $\bar{\Gamma}$  is the boundary of an open set  $E$  and we denote by  $T$  the open set delimited by the half-lines  $L_-, L_+$  which agrees with  $E$  outside  $B$  (see Figure 2), then a modification of the computation in (ii) gives

$$\int_{\bar{\Gamma}} \bar{v} d\sigma = \pm (|E \cap B| - |T \cap B|).$$

In particular assumption (4.11) is equivalent to saying that  $E \cap B$  and  $T \cap B$  have the same area, which means that  $(E \setminus T) \cap B$  and  $(T \setminus E) \cap B$  have the same area (see Figure 2).

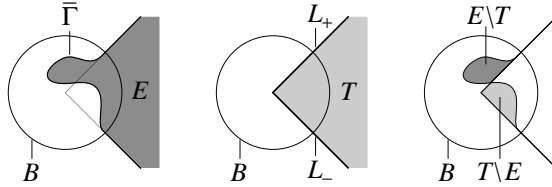


FIGURE 2. The situation described in Remark 4.10(iii).

The rest of this section is devoted to the proofs of Propositions 4.6 and 4.9. The key step is contained in Lemma 4.12.

**4.11. Potential of a velocity field.** Let  $u : \mathbb{R}^2 \rightarrow \mathbb{R}^2$  be a continuous velocity field and let  $\varphi : \mathbb{R}^2 \rightarrow \mathbb{R}$  be a function of class  $C^1$ . We say that  $\varphi$  is a *potential* for  $u$  if

$$u = \nabla^\perp \varphi,$$

where  $\nabla^\perp := (-\partial_2, \partial_1)$ . Note that  $u$  admits a potential if and only if it is divergence-free. In the fluid dynamics literature, such  $\varphi$  is called a stream function for the flow generated by  $u$ .



**Lemma 4.12.** *Let  $\Gamma$  be a curve and  $v$  be a function on the curve  $\Gamma$ , both of class  $C^k$  with  $k \geq 2$ . Given a positive number  $\bar{r}$  and a compact (not necessarily proper) sub-arc  $G$  of  $\Gamma$ , which contains the support of  $v$ , assume that*

$$\int_{\Gamma} v d\sigma = 0. \quad (4.12)$$

*Then there exists a divergence-free, autonomous velocity field  $u$  on  $\mathbb{R}^2$  of class  $C^{k-2}$ , the normal component of which on  $\Gamma$ , that is  $u \cdot \eta$ , agrees with  $v$ , and the support of which is contained in  $B(G, \bar{r})$ .*

**Proof.** We describe the proof in the case  $J = \mathbb{R}$ , where we recall that  $J$  is the domain of the parametrization of the curve  $\Gamma$ ; the case  $J = \mathbb{T}^1$  requires few straightforward modifications. In view of §4.11, it suffices to find a potential  $\varphi : \mathbb{R}^2 \rightarrow \mathbb{R}$  of class  $C^{k-1}$  and with support contained in  $B(G, \bar{r})$  such that

$$\partial_{\tau} \varphi = v \quad \text{on } \Gamma, \quad (4.13)$$

where  $\tau$  is the tangent vector to  $\Gamma$ , and then take  $u := \nabla^{\perp} \varphi$ .

Let  $\gamma : \mathbb{R} \rightarrow \mathbb{R}^2$  be a parametrization of  $\Gamma$ . For the construction of  $\varphi$  we choose

- a point  $x_0 = \gamma(s_0) \in \Gamma$  and, if  $G$  is a proper sub-arc of  $\Gamma$ , we further require that  $x_0$  does not belong to  $G$ ;
- a smooth function  $g : \mathbb{R} \rightarrow \mathbb{R}$  with support contained in  $[-1/2, 1/2]$  such that  $g(0) = 1$ ;
- a number  $0 < r < \bar{r}$  smaller than the tubular radius of  $\Gamma$ .

Now we take the diffeomorphism  $\Psi : \mathbb{R} \times (-r, r) \rightarrow B(\Gamma, r)$  defined in (4.1), and for every  $x = \Psi(s, y) \in B(\Gamma, r)$  we set

$$\varphi(x) = \varphi(\Psi(s, y)) := g(y/r) \int_{s_0}^s v(\gamma(s')) |\dot{\gamma}(s')| ds'. \quad (4.14)$$

If  $x$  belongs to  $\Gamma$  then  $x = \gamma(s) = \Psi(s, 0)$ , and therefore  $\varphi(x)$  is the integral of  $v$  along the (oriented) sub-arc of  $\Gamma$  starting from  $x_0$  and ending at  $x$ . Thus the restriction of  $\varphi$  to  $\Gamma$  is a primitive of  $v$ , and therefore it satisfies (4.13).

Now, formula (4.14) shows that  $\varphi \circ \Psi$  is a function of class  $C^k$  on  $\mathbb{R} \times (-r, r)$  with support contained in  $\mathbb{R} \times [-r/2, r/2]$ , and since  $\Psi$  is a diffeomorphism of class  $C^{k-1}$  and maps  $\mathbb{R} \times [-r/2, r/2]$  into the closure of  $B(\Gamma, r/2)$ , we deduce that  $\varphi$  is a function of class  $C^{k-1}$  on  $B(\Gamma, r)$  with support contained in the closure of  $B(\Gamma, r/2)$ .

We complete the construction by extending  $\varphi$  to 0 in the rest of  $\mathbb{R}^2$ .

It remains to check that the support of  $\varphi$  is contained in  $B(G, \bar{r})$ . When  $G = \Gamma$ , this follows by the fact that the support of  $\varphi$  is contained in the closure of  $B(\Gamma, r/2)$ , which is contained in  $B(\Gamma, \bar{r})$ . When  $G = \gamma([s_1, s_2])$  is a proper sub-arc of  $\Gamma$  we have that

- $v(\gamma(s)) = 0$  for  $s \notin [s_1, s_2]$  by assumption;
- $s_0 \notin [s_1, s_2]$  by the choice of  $x_0$ ;

- condition (4.12) can be re-written as  $\int_{s_1}^{s_2} v(\gamma(s')) |\dot{\gamma}(s')| ds' = 0$ .

Putting together these facts and recalling the choice of  $g$  one easily shows that  $\varphi(\Psi(s, y)) = 0$  if  $s \notin [s_1, s_2]$  or  $y \notin [-r/2, r/2]$ , and then

$$\text{supp}(\varphi) \subset \Psi([s_1, s_2] \times [-r/2, r/2]) \subset B(G, \bar{r}). \quad \square$$

**Proof of Proposition 4.9.** Statement (i) follows from Lemma 4.12, while statement (ii) is an immediate consequence of statement (i) and §4.8.  $\square$

**Proof of Proposition 4.6.** For every  $t \in I$  we use Lemma 4.12 to construct a divergence-free velocity field  $u(t, \cdot)$  of class  $C^{k-2}$  which satisfies the compatibility condition (4.2) at time  $t$ , and whose support is contained in  $B(G(t), \bar{r}(t))$ .

However, this only gives that  $u$  is of class  $C^{k-2}$  in the variable  $x$ . To show that  $u$  can be taken of class  $C^{k-2}$  in  $t$  and  $x$ , we must go through the proof of Lemma 4.12. In doing so we quickly realize that the key point is the regularity of class  $C^{k-1}$  in the variables  $t, s, y$  of the right-hand side of formula (4.14), that in our specific case is

$$g(y/r(t)) \int_{s_0(t)}^s v_n(t, \gamma(t, s')) |\dot{\gamma}(t, s')| ds'.$$

It is clear that this quantity has the required regularity provided that we choose  $r(t)$  and  $s_0(t)$  at least of class  $C^{k-1}$  in  $t$ .

Since both  $\bar{r}(t)$  and the tubular radius of  $\Gamma(t)$  are continuous, strictly positive functions of  $t$ , it is always possible to choose  $r(t)$  smaller than both, strictly positive, and smooth in  $t$ .

If we only require that the support of  $u$  is contained in  $B(\Gamma(t), \bar{r}(t))$ , we can take  $s_0(t)$  constant in  $t$ . If we require that the support of  $u$  is contained in  $B(G(t), \bar{r}(t))$ , then we can again choose  $s_0(t)$  smooth in  $t$ , but this choice is more delicate, and relies on the fact that  $G(t)$  is a proper sub-arc for all  $t \in I$ .  $\square$

## 5. FIRST EXAMPLE: PINCHING

In this section we verify Assumption 3.1 for  $s = 1$  and for every  $1 \leq p < \infty$ . In fact, we do this by constructing a velocity field and a solution on  $\mathbb{R}^2$ , both compactly supported in the open unit square  $\mathcal{Q}$ , for every  $s$  and  $p$  such that  $p$  is strictly below the critical exponent for the embedding of  $W^{s,p}$  in the Lipschitz class, that is,

$$s < 1 \text{ and } p \leq \infty, \text{ or } s \geq 1 \text{ and } p < \frac{2}{s-1}. \quad (5.1)$$

More precisely, we give an example of a velocity field  $u_0$  and a solution  $\rho_0$  of the continuity equation (1.1), both defined for  $0 \leq t \leq 1$ , such that

- (a)  $u_0$  is a time-dependent velocity field on  $\mathbb{R}^2$ , compactly supported in the open unit square  $\mathcal{Q}$ , smooth in both variables for  $t \neq k/8$  with  $k = 1, \dots, 7$ , bounded, divergence-free, and bounded in  $\dot{W}^{s,p}(\mathbb{R}^2)$  uniformly in  $t$  for all  $s, p$  as above;

- (b)  $\rho_0$  is of the form  $\rho_0(t, \cdot) = 1_{E(t)} - \pi/16$  where  $E(t)$  is a time-dependent domain in  $\mathbb{R}^2$  defined for  $0 \leq t \leq 1$ , continuous for all  $t$ ,<sup>16</sup> smooth for  $t \neq k/8$  with  $k = 1, \dots, 7$ , with closure contained in  $\mathcal{Q}$ , and area equal to  $\pi/16$  (thus  $\rho_0(t, \cdot)$  has average zero).
- (c)  $E(0)$  is the disk with center 0 and radius  $1/4$  while  $E(1)$  is the union of the four disks with centers  $(\pm 1/4, \pm 1/4)$  and radius  $1/8$ .

Since  $u_0$  and  $\rho_0$  have compact support in the open square  $\mathcal{Q}$  we can see them as a velocity field and a solution on the torus  $\mathbb{T}^2$ . For  $s = 1$ , the locality of the distributional derivative of order 1 ensures that  $u_0$  is bounded in  $\dot{W}^{1,p}(\mathbb{T}^2)$  for every  $1 \leq p < \infty$ . Therefore Assumption 3.1 is satisfied for  $s = 1$  and for every  $1 \leq p < \infty$ .

As a matter of fact, we construct a time-dependent domain  $E$  as above and a velocity field  $u_0$  defined for  $t \neq k/8$  with  $k = 1, \dots, 7$ , which is smooth and compatible with  $E$ . This ensures that the characteristic function  $1_{E(t)}$  is a distributional solution of the continuity equation (1.1) in the open time intervals  $((k-1)/8, k/8)$  with  $k = 1, \dots, 8$ ; the fact that it is also a solution on the time interval  $[0, 1]$  is ensured by the continuity in  $t$  (recall Footnote 12). The set  $E(t)$  for  $t = k/8$  with  $k = 0, \dots, 4$  and  $t = 1$  is described in Figure 3.

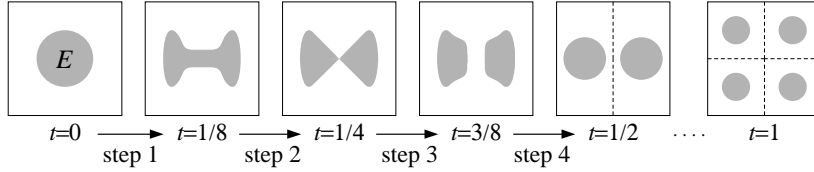


FIGURE 3. The set  $E(t)$  for  $t = k/8$  with  $k = 0, \dots, 4$  and  $t = 1$ .

More precisely, we denote by  $B$  the open disk with center 0 and radius  $1/4$ , by  $T$  the cone of all  $x \in \mathbb{R}^2$  such that  $|x_2| < |x_1|$ , and for  $t = 1/8$ ,  $t = 1/4$ , and  $t = 3/8$  we require that

- (d)  $E(t)$  is symmetric w.r.t. both axes;
- (e) the set  $E(t)$  has area  $\pi/16$ ;
- (f) the set  $E(t) \setminus B$  is the same, that is, is left invariant by the flow;
- (g) the sets  $(E(1/8) \setminus T) \cap B$  and  $(T \setminus E(1/8)) \cap B$  have the same area.

In the rest of this section we describe the construction of  $E(t)$  and  $u_0(t, \cdot)$  for  $t$  in the time intervals  $[0, 1/8]$  (Step 1 in Figure 3) and  $(1/8, 1/4)$  (Step 2 in Figure 3). The construction in the remaining time intervals (steps) is similar, and is omitted.

*Step 1: construction of  $E(t)$  and  $u_0(t, \cdot)$  for  $0 \leq t \leq 1/8$ .* Since  $E(0)$  and  $E(1/8)$  are both smooth and have area  $\pi/16$ , we can clearly find  $E(t)$  for  $0 < t < 1/8$  with

<sup>16</sup> Or more precisely,  $t \mapsto 1_{E(t)}$  is continuous as a map with values, say, in  $L^1(\mathbb{R}^2)$ .

area  $\pi/16$  so that  $t \mapsto E(t)$  is smooth on  $[0, 1/8]$ . Then by Proposition 4.6 we can find a smooth velocity field  $u_0 : [0, 1/8] \times \mathbb{R}^2 \rightarrow \mathbb{R}^2$  which is divergence-free and compatible with  $E$ . Moreover, since  $\partial E(t)$  is contained in  $\mathcal{Q}$ , we can assume that the support of  $u_0$  is contained in  $\mathcal{Q}$  for all  $t$ . In particular, all positive Sobolev norms of  $u_0(t, \cdot)$  are uniformly bounded in  $t$ .

*Step 2: construction of  $E(t)$  and  $u_0(t, \cdot)$  for  $1/8 < t < 1/4$ .* Let  $\bar{\Gamma}$  be the proper curve drawn in Figure 4. More precisely,  $\bar{\Gamma}$  is defined outside  $B$  by the equation  $x_2 = |x_1|$ , and agrees in  $B$  with the “upper” connected component of  $\partial E(1/8) \cap B$ .

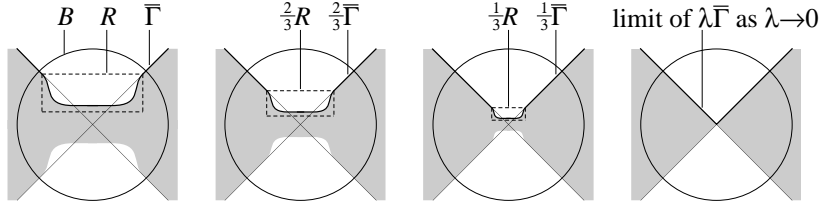


FIGURE 4. The curve  $\bar{\Gamma}$ , the homothetic copies  $\lambda \bar{\Gamma}$  with  $\lambda = 2/3$ ,  $\lambda = 1/3$ , and their limit as  $\lambda \rightarrow 0$ .

We consider a decreasing smooth function  $\lambda$  on  $[1/8, 1/4)$  such that  $\lambda(1/8) = 1$  and  $\lambda(t)$  tends to 0 as  $t \rightarrow 1/4$ ; the function  $\lambda$  will be explicitly chosen later in order to satisfy further requirements. Then we take  $E(t)$  for all  $1/8 < t < 1/4$  satisfying the following requirements:

- (h)  $E(t)$  agrees with  $E(1/8)$  outside  $B$ ;
- (i)  $\partial E(t) \cap B$  has two connected component which are symmetric with respect to the  $x_1$  axis, and the upper one agrees with  $\lambda(t) \bar{\Gamma}$  in  $B$ ; thus  $E(t) \cap B$  is described in Figure 4 when  $\lambda(t) = 1$ ,  $\lambda(t) = 2/3$ , and  $\lambda(t) = 1/3$ .

By Remark 4.10(iii), assumption (g) above implies that the curve  $\bar{\Gamma}$  satisfies condition (4.11), and therefore we can use Proposition 4.9(ii) to obtain a smooth, divergence-free velocity field  $u : [1/8, 1/4) \times \mathbb{R}^2 \rightarrow \mathbb{R}^2$  which is compatible with the homothetic curve  $\lambda(t) \bar{\Gamma}$ . Moreover  $u(t, \cdot)$  is compactly supported in the upper half-plane  $\mathbb{R} \times (0, +\infty)$  for all  $t$  (more precisely, we can require that the support is contained in the dashed rectangle  $R$  in Figure 4).

Finally we take  $u_0 : [1/8, 1/4) \times \mathbb{R}^2 \rightarrow \mathbb{R}^2$  equal to  $u$  in the upper half-plane, and we extend it to the lower half-plane by reflection. Thus  $u_0$  is still smooth and compactly supported, and by assumption (i) above is compatible with the time-dependent domain  $E$  inside the ball  $B$ . On the other hand,  $u_0$  vanishes outside the ball  $B$  and therefore it is compatible with the set  $E \setminus B$ , which is constant in time (recall assumption (g)). In conclusion,  $u_0$  is compatible with  $E$ .

It remains to choose  $\lambda$  so that  $u_0(t, \cdot)$  is bounded in  $\dot{W}^{s,p}(\mathbb{R}^2)$  uniformly in  $t \in [1/8, 1/4)$  for every  $s, p$  as in (5.1). To this end, we recall that by Proposition 4.9(ii) the field  $u_0$  can be written in the form

$$u_0(t, x) = \lambda'(t) \bar{u}(x/\lambda(t))$$

where  $\bar{u} : \mathbb{R}^2 \rightarrow \mathbb{R}^2$  is smooth and compactly supported. Therefore, using (2.8), for every  $t$  we obtain

$$\|u_0(t, \cdot)\|_{\dot{W}^{s,p}(\mathbb{R}^2)} = |\lambda'(t)| |\lambda(t)|^{2/p-s} \|\bar{u}\|_{\dot{W}^{s,p}(\mathbb{R}^2)}.$$

Now, a simple computation shows that  $u_0(t, \cdot)$  is uniformly bounded in  $\dot{W}^{s,p}(\mathbb{R}^2)$  if we take

$$\lambda(t) := \exp\left(2 - \frac{1}{1-4t}\right).$$

With this choice of the function  $\lambda(t)$  the velocity field  $u_0(t, \cdot)$  is also bounded.

*Remark 5.1.* (i) The flow of the (non-Lipschitz) velocity field  $u_0$  changes the topology of sets: the ball at time  $t = 0$  is transformed into two balls at time  $t = 1/2$ .

(ii) Using symmetry considerations, it is possible to check that the flow of  $u_0$  shrinks from time  $t = 1/8$  to time  $t = 1/4$  a vertical segment to the origin (which is represented by the intersection of the two lines in Figure 4).

(iii) Analogously, from time  $t = 1/4$  to time  $t = 3/8$  the flow of  $u_0$  “spreads” the origin over an horizontal segment. In particular, the ODE with velocity field  $u_0$  and initial time  $t = 1/8$  does not have (pointwise) uniqueness for all initial data laying on the vertical segment described in (ii) above.

## 6. SCALING ANALYSIS IN A QUASI SELF-SIMILAR CONSTRUCTION

A velocity field behaving like the one constructed in Section 5 cannot have Lipschitz regularity, since the associated evolution does not preserve the connectedness of sets. Indeed, it is not evident that Assumption 3.1 can be satisfied with  $s = 1$  and  $p = \infty$ . In this section we address this case by replacing the (exactly) self-similar procedure in Section 3 by a *quasi self-similar* procedure. That is, instead of replicating rescaled copies of *one* basic element at each step of the evolution (as in §3.3), we consider a *finite family* of basic elements, which are rescaled and rearranged at each step of the evolution according to a combinatorial pattern. We implement this construction on the plane  $\mathbb{R}^2$ .

Given  $s > 0$  and  $1 \leq p \leq \infty$ , Assumption 3.1 is replaced by the assumption below, where we denote by  $\lceil s \rceil$  the smallest integer greater or equal than  $s$ . We also recall that, for  $p = \infty$ , the space  $\dot{W}^{s,\infty}$  is a Lipschitz-Hölder space, discussed in §2.5.

**6.1. Assumption. Almost self-similar basic family.** For  $j = 1, \dots, N$  there exist velocity fields  $u^j$  and corresponding (not identically zero) solutions  $\rho^j$  to (1.1), all defined for  $0 \leq t \leq 1$  and  $x \in \mathbb{R}^2$ , such that:

- (i) each  $w^j$  is bounded in  $\dot{W}^{[s],p}(\mathbb{R}^2)$  uniformly in time, bounded, divergence-free, and tangent to  $\partial\mathcal{Q}$ ;<sup>17</sup>
- (ii) each  $\rho^j$  is bounded and has zero average on  $\mathcal{Q}$ ;
- (iii) there exists a positive constant  $\lambda$ , with  $1/\lambda$  an integer greater or equal than 2, such that each function  $\rho^j(1, \cdot)$  agrees on each square of the tiling  $\mathcal{T}_\lambda$  (recall Definition 3.2) with a rescaled translation of one of the functions  $\{\rho^i(0, \cdot)\}_{1 \leq i \leq N}$ , in the sense that for each  $Q \in \mathcal{T}_\lambda$

$$\rho^j(1, x) = \rho^{\gamma(j, Q)} \left( 0, \frac{x - r_Q}{\lambda} \right) \quad \text{for } x \in Q,$$

for suitable  $\gamma = \gamma(j, Q) \in \{1, \dots, N\}$ .

For later use, for any  $\sigma \geq 0$  we set

$$M_\sigma := \max_{j=1, \dots, N} \sup_{0 \leq t \leq 1} \|\rho^j(t, \cdot) 1_{\mathcal{Q}}\|_{\dot{H}^{-\sigma}(\mathbb{R}^2)}. \quad (6.1)$$

Since each  $\rho^j$  is bounded and has zero average on  $\mathcal{Q}$ , it follows from Remark 2.2(iv) that  $M_\sigma$  is finite for  $0 \leq \sigma < 2$ .

**6.2. Quasi self-similar construction.** Under Assumption 6.1 we now define inductively a quasi self-similar evolution.

*Initial step.* We start by choosing a positive constant  $\bar{\lambda}$ , with  $1/\bar{\lambda}$  an integer greater or equal than 1.<sup>18</sup> We define the evolution for  $0 \leq t \leq 1$  by patching together velocity fields and solutions on the tiling  $\mathcal{T}_{\bar{\lambda}}$  of  $\mathcal{Q}$ .

For every  $Q \in \mathcal{T}_{\bar{\lambda}}$  we choose an index  $\bar{j}(Q) \in \{1, \dots, N\}$  and we set for  $x \in Q$  and  $0 \leq t \leq 1$

$$u(t, x) := \bar{\lambda} u^{\bar{j}(Q)} \left( t, \frac{x - r_Q}{\bar{\lambda}} \right), \quad \rho(t, x) := \rho^{\bar{j}(Q)} \left( t, \frac{x - r_Q}{\bar{\lambda}} \right). \quad (6.2)$$

For  $x \notin \mathcal{Q}$  we set both  $u$  and  $\rho$  equal to zero.

We stress that, in this construction (as well as in the one in the iterative step below), the resulting field is divergence-free, but it does not necessarily have Sobolev regularity as the derivative may jump at the boundary of the patch. In what follows, we will *assume* the needed regularity (see Assumption 6.3 below). We will prove later that this assumption is satisfied in the example we give in Section 8.

Since the velocity field  $u$  in (6.2) is tangent to all the interfaces of the tiling  $\mathcal{T}_{\bar{\lambda}}$  it follows that  $\rho$  in (6.2) solves the continuity equation with velocity field  $u$  globally in  $\mathbb{R}^2$ . We notice that, by Assumption 6.1(iii), on each square of the tiling  $\mathcal{T}_{\bar{\lambda}}$  the function  $\rho(1, \cdot)$  equals a rescaled translation of one of the functions  $\{\rho^i(0, \cdot)\}_{1 \leq i \leq N}$ .

<sup>17</sup> Notice that the normal trace of  $w^j$  on  $\partial\mathcal{Q}$  (both from inside and from outside) is well defined in distributional sense.

<sup>18</sup> Here we allow  $\bar{\lambda} = 1$ .

*Iterative step.* For a given positive parameter  $\tau$  to be chosen later, we define as in §3.3

$$T_n := \sum_{i=0}^{n-1} \tau^i, \quad \text{for } n = 1, 2, \dots, \infty.$$

We now assume that  $u$  and  $\rho$  have been defined for  $0 \leq t \leq T_n$ , in such a way that on each square of the tiling  $\mathcal{T}_{\bar{\lambda}\lambda^n}$  the function  $\rho(T_n, \cdot)$  equals a rescaled translation of one of the functions  $\{\rho^i(0, \cdot)\}_{1 \leq i \leq N}$ , and we show how to define  $u$  and  $\rho$  for  $T_n < t \leq T_{n+1}$ .

Consider a square  $Q \in \mathcal{T}_{\bar{\lambda}\lambda^n}$ . By the inductive assumption there exists an index  $j = j(n, Q)$  such that

$$\rho(T_n, x) = \rho^j \left( 0, \frac{x - r_Q}{\bar{\lambda}\lambda^n} \right) \quad \text{for } x \in Q. \quad (6.3)$$

Accordingly we define for  $x \in Q$  and  $T_n < t \leq T_{n+1}$

$$u(t, x) := \frac{\bar{\lambda}\lambda^n}{\tau^n} u^j \left( \frac{t - T_n}{\tau^n}, \frac{x - r_Q}{\bar{\lambda}\lambda^n} \right), \quad \rho(t, x) := \rho^j \left( \frac{t - T_n}{\tau^n}, \frac{x - r_Q}{\bar{\lambda}\lambda^n} \right). \quad (6.4)$$

As before, for  $x \notin \mathcal{Q}$  we set both  $u$  and  $\rho$  equal to zero. By the same argument as in the initial step, we have that for  $T_n < t \leq T_{n+1}$  the function  $\rho$  in (6.4) solves the continuity equation with velocity field  $u$  globally in  $\mathbb{R}^2$ .

By Assumption 6.1(iii), on each square of the tiling  $\mathcal{T}_{\bar{\lambda}\lambda^{n+1}}$  the function  $\rho(T_{n+1}, \cdot)$  equals a rescaled translation of one of the functions  $\{\rho^i(0, \cdot)\}_{1 \leq i \leq N}$ . This concludes the inductive procedure, which gives a velocity field  $u$  and a solution  $\rho$  of (1.1) defined for a.e.  $x \in \mathbb{R}^2$  and for all  $t \geq 0$ .

We now make a further assumption on the velocity fields  $u$  constructed in the quasi-self similar manner. One drawback of our construction, in fact, is that we do not control (at least a priori) the behavior of derivatives of the field at the boundary of each patch. We are therefore forced at this stage to make a further assumption on  $u$ , regarding its regularity. This assumption will be proved to be satisfied in the example we give in Section 8.

**6.3. Assumption. Regularity of the patching.** For a.e.  $t \geq 0$  we have that  $u(t, \cdot) \in \dot{W}^{[s], p}(\mathbb{R}^2)$ .

*Remark 6.4.* (i) The fact that Assumptions 6.1 and 6.3 entail regularity of order  $[s]$  (rather than  $s$ ) is technical and due to the fact that the norm on Sobolev spaces with integer order is local, property that we will exploit in the proof of Lemma 6.5.

(ii) Assumption 6.3 is, in fact, the key structural condition to ensure a quasi self-similar construction yields fields of the required regularity, as already observed above. It is indeed easy to construct families of velocity fields and solutions that satisfy Assumption 6.1 without verifying Assumption 6.3. We will construct a family that satisfies both assumptions, for any  $s$  and  $p$  in Section 8.

(iii) In the relevant case  $s = 1$  and  $p = \infty$ , i.e., in the Lipschitz case, Assumption 6.3 can be rephrased as requiring that  $u$  have a continuous representative on  $\mathbb{R}^2$  (and actually it is sufficient to check the continuity of  $u$  on the boundaries of the sub-squares in the tilings).

We stress that we do not require any uniformity of the Sobolev norm with respect to time in Assumption 6.3. Under this assumption, the uniformity in time is in fact guaranteed by the following lemma, provided we choose  $\tau$  as in §3.3.

**Lemma 6.5.** *Let  $\tau = \lambda^{1-s}$ . Under Assumptions 6.1 and 6.3, the velocity field  $u$  constructed by the quasi self-similar procedure in §6.2 is divergence-free and belongs to  $\dot{W}^{s,p}(\mathbb{R}^2)$  uniformly in time.*

**Proof.** First of all, since each velocity field  $u^j$  is divergence-free in  $\mathcal{Q}$  and tangent to the boundary  $\partial\mathcal{Q}$ , it follows that  $u$  is divergence-free. It remains to prove the bound in  $\dot{W}^{s,p}(\mathbb{R}^2)$ .

*Step 1: the case  $s = k$  an integer.* Consider  $T_n < t \leq T_{n+1}$ . Then  $u(t, \cdot)$  is defined as in (6.4) for some function  $j = j(n, Q)$ . Assumption 6.3 guarantees that  $u(t, \cdot) \in \dot{W}^{k,p}(\mathbb{R}^2)$ , therefore (by the absolute continuity of the derivative of a Sobolev function of integer order) we only need to estimate the sum of the  $\dot{W}^{k,p}$  norms of the restriction of  $u(t, \cdot)$  to the squares  $Q$  in  $\mathcal{T}_{\bar{\lambda}\lambda^n}$ . We can compute as follows:

$$\begin{aligned} \|u(t, \cdot)\|_{\dot{W}^{k,p}(\mathbb{R}^2)}^p &= \int_{\mathcal{Q}} |\nabla^k u(t, x)|^p dx \\ &= \sum_{Q \in \mathcal{T}_{\bar{\lambda}\lambda^n}} \int_Q \left| \nabla^k \left( \frac{\bar{\lambda}\lambda^n}{\tau^n} u^j \left( \frac{t - T_n}{\tau^n}, \frac{x - r_Q}{\bar{\lambda}\lambda^n} \right) \right) \right|^p dx \\ &= \sum_{Q \in \mathcal{T}_{\bar{\lambda}\lambda^n}} \int_Q \left| \frac{\bar{\lambda}\lambda^n}{\tau^n \bar{\lambda}^k \lambda^{kn}} (\nabla^k u^j) \left( \frac{t - T_n}{\tau^n}, \frac{x - r_Q}{\bar{\lambda}\lambda^n} \right) \right|^p dx \\ &= \left( \frac{\lambda^{1-k}}{\tau} \right)^{pn} \bar{\lambda}^{p(1-k)} \sum_{Q \in \mathcal{T}_{\bar{\lambda}\lambda^n}} \int_{\mathcal{Q}} \left| (\nabla^k u^j) \left( \frac{t - T_n}{\tau^n}, y \right) \right|^p (\bar{\lambda}\lambda^n)^2 dy \\ &\leq \left( \frac{\lambda^{1-k}}{\tau} \right)^{pn} \bar{\lambda}^{p(1-k)} \max_{1 \leq j \leq N} \sup_{0 \leq r \leq 1} \|u^j(r, \cdot)\|_{\dot{W}^{k,p}(\mathbb{R}^2)}^p. \end{aligned}$$

The computation for  $p = \infty$  is analogous, considering the supremum norm, and gives

$$\|u(t, \cdot)\|_{\dot{W}^{k,\infty}(\mathbb{R}^2)} \leq \left( \frac{\lambda^{1-k}}{\tau} \right)^n \bar{\lambda}^{(1-k)} \max_{1 \leq j \leq N} \sup_{0 \leq r \leq 1} \|u^j(r, \cdot)\|_{\dot{W}^{k,\infty}(\mathbb{R}^2)}.$$

The choice  $\tau = \lambda^{1-s}$  concludes the proof for  $s = k$  integer.



*Step 2: the general case  $s \geq 0$  a real.* We rely on the previous step and we use (2.11) with  $s_1 = \lceil s \rceil$ ,  $s_2 = 0$  and  $\vartheta = s/\lceil s \rceil$ , getting

$$\begin{aligned} \|u(t, \cdot)\|_{\dot{W}^{s,p}(\mathbb{R}^2)} &\leq \|u(t, \cdot)\|_{L^p(\mathbb{R}^2)}^{1-\vartheta} \|u(t, \cdot)\|_{\dot{W}^{\lceil s \rceil,p}(\mathbb{R}^2)}^{\vartheta} \\ &\leq \left(\frac{\lambda}{\tau}\right)^{(1-\vartheta)n} \bar{\lambda}^{1-\vartheta} \left(\frac{\lambda^{1-\lceil s \rceil}}{\tau}\right)^{\vartheta n} \bar{\lambda}^{(1-\lceil s \rceil)\vartheta} \\ &\quad \times \max_{1 \leq j \leq N} \sup_{0 \leq r \leq 1} \left[ \|u^j(r, \cdot)\|_{L^p(\mathbb{R}^2)} + \|u^j(r, \cdot)\|_{\dot{W}^{\lceil s \rceil,p}(\mathbb{R}^2)} \right] \\ &= \left(\frac{\lambda^{1-s}}{\tau}\right)^n \bar{\lambda}^{1-s} \max_{1 \leq j \leq N} \sup_{0 \leq r \leq 1} \left[ \|u^j(r, \cdot)\|_{L^p(\mathbb{R}^2)} + \|u^j(r, \cdot)\|_{\dot{W}^{\lceil s \rceil,p}(\mathbb{R}^2)} \right], \end{aligned}$$

where we have used the estimate in Step 1 with  $k = 0$  and  $k = \lceil s \rceil$ . Again the choice  $\tau = \lambda^{1-s}$  allows to conclude.  $\square$

**6.6. Decay of the functional mixing norm.** We now analyze the behavior in time of negative Sobolev norms of the solution  $\rho$  constructed in §6.2. For  $T_n \leq t < T_{n+1}$  we have

$$\rho(t, x) = \sum_{Q \in \mathcal{T}_{\bar{\lambda}\lambda^n}} \rho^j \left( \frac{t - T_n}{\tau^n}, \frac{x - r_Q}{\bar{\lambda}\lambda^n} \right) 1_Q(x) \quad \text{for } x \in \mathbb{R}^2,$$

for a suitable  $j = j(n, Q)$ . For any  $r > 0$ , equation (2.9) implies that

$$\begin{aligned} \|\rho(t, \cdot)\|_{\dot{H}^{-r}(\mathbb{R}^2)} &\leq \sum_{Q \in \mathcal{T}_{\bar{\lambda}\lambda^n}} \left\| \rho^j \left( \frac{t - T_n}{\tau^n}, \frac{x - r_Q}{\bar{\lambda}\lambda^n} \right) 1_Q(x) \right\|_{\dot{H}^{-r}(\mathbb{R}^2)} \\ &= \sum_{Q \in \mathcal{T}_{\bar{\lambda}\lambda^n}} \bar{\lambda}^{1+r} \lambda^{n(1+r)} \left\| \rho^j \left( \frac{t - T_n}{\tau^n}, \cdot \right) 1_{\mathcal{Q}} \right\|_{\dot{H}^{-r}(\mathbb{R}^2)} \\ &\leq \bar{\lambda}^{1+r} \frac{\lambda^{n(1+r)}}{\lambda^{2n}} M_r = \bar{\lambda}^{1+r} \lambda^{n(r-1)} M_r, \quad \text{for } T_n \leq t < T_{n+1}, \end{aligned} \tag{6.5}$$

with  $M_r$  as in (6.1). Using (2.10) we find that, for every  $\gamma \geq 1$ ,

$$\|\rho(t, \cdot)\|_{\dot{H}^{-\sigma}(\mathbb{R}^2)} \leq \|\rho(t, \cdot)\|_{\dot{H}^{-\gamma\sigma}(\mathbb{R}^2)}^{1/\gamma} \|\rho(t, \cdot)\|_{L^2(\mathbb{R}^2)}^{1-1/\gamma}. \tag{6.6}$$

Now, given  $\sigma$ , choose  $\gamma \geq 1$  such that  $1 < \sigma\gamma < 2$ . This is indeed possible as long as  $0 < \sigma < 2$ . Then (6.6), together with (6.5) for  $r = \gamma\sigma$  gives

$$\|\rho(t, \cdot)\|_{\dot{H}^{-\sigma}(\mathbb{R}^2)} \leq \bar{\lambda}^{\sigma+1/\gamma} M_0^{1-1/\gamma} M_{\gamma\sigma}^{1/\gamma} \lambda^{n(\sigma-1/\gamma)}, \quad \text{for } T_n \leq t < T_{n+1}, \tag{6.7}$$

owing to the fact that the  $L^2$  norm of the solution is conserved for all  $t \geq 0$ :

$$\|\rho(t, \cdot)\|_{L^2(\mathbb{R}^2)} = M_0.$$

Finally, setting

$$c_\sigma := \sigma - 1/\gamma > 0, \quad C_\sigma := \bar{\lambda}^{\sigma+1/\gamma} M_0^{1-1/\gamma} M_{\gamma\sigma}^{1/\gamma} > 0,$$

Equation (6.7) becomes

$$\|\rho(t, \cdot)\|_{\dot{H}^{-\sigma}(\mathbb{R}^2)} \leq C_\sigma \lambda^{nc_\sigma}, \quad \text{for } T_n \leq t < T_{n+1}. \quad (6.8)$$

In particular, for  $\sigma = 1$ , choosing  $\gamma = 3/2$  yields:

$$\|\rho(t, \cdot)\|_{\dot{H}^{-1}(\mathbb{R}^2)} \leq \bar{\lambda}^{5/3} M_0^{1/3} M_{3/2}^{2/3} \lambda^{n/3}, \quad \text{for } T_n \leq t < T_{n+1}. \quad (6.9)$$

The above estimates (6.8) and (6.9) corresponds to (3.2) in §3.3. Therefore, arguing as in the final step of the proof of Theorem 3.4, we obtain the following result.

**Theorem 6.7.** *Given  $s > 0$  and  $1 \leq p \leq \infty$ , under Assumptions 6.1 and 6.3, there exist a bounded, divergence-free velocity field  $u$  and a solution  $\rho$  of the Cauchy problem for (1.1) in  $\mathbb{R}^2$ , such that  $u$  is bounded in  $\dot{W}^{s,p}(\mathbb{R}^2)$  uniformly in time,  $u$  and  $\rho$  are supported in  $\mathcal{Q}$  for all times, and the functional mixing scale of  $\rho$  exhibits the following behavior depending on  $s$ :*

- (1) *Case  $s < 1$ : perfect mixing in finite time;*
- (2) *Case  $s = 1$ : exponential decay;*
- (3) *Case  $s > 1$ : polynomial decay.*

*Remark 6.8.* (i) In fact, in the case  $s = 1$ , every  $\dot{H}^{-\sigma}$  norm of  $\rho$  decays exponentially in time for  $0 < \sigma < 2$  (see (6.8)). Moreover, if  $M_{\tilde{\sigma}} < \infty$  for some  $\tilde{\sigma} \geq 2$ , where  $M_\sigma$  is given in (6.1), then every  $\dot{H}^{-\sigma}$  norm of  $\rho$  decays exponentially in time for  $0 < \sigma < \tilde{\sigma}$ .

(ii) Thanks to Lemma 3.5 we can deduce that the geometric mixing scale  $\varepsilon(t)$  of  $\rho(t, \cdot)$  exhibits the same behavior of the functional mixing scale detailed in Theorem 6.7.

(iii) For later use (in the companion paper [3]) we make here the following observation. In the case  $s = 1$ , Theorem 6.7 provides a velocity field  $u$  bounded in  $\dot{W}^{1,p}(\mathbb{R}^2)$  uniformly in time and a solution  $\rho$  of the continuity equation for which the functional mixing scale decays exponentially in time. In addition, for any real number  $r \geq 0$ , such a velocity field satisfies

$$\|u(t, \cdot)\|_{\dot{W}^{r,p}(\mathbb{R}^2)} \leq C_r (\lambda^{1-r})^t.$$

This estimates follows from the proof of Lemma 6.5 (recalling that in this case  $\tau = 1$ ). In particular, the Sobolev norms of  $u$  of order higher than one grow exponentially in time, while the Sobolev norms of order lower than one decay exponentially in time.

(iv) In the case when  $s$  is a positive integer, the fact that the velocity field and the solution are supported in  $\mathcal{Q}$  and the locality of the distributional derivative of positive integer order imply the validity of Theorem 6.7 with domain the torus  $\mathbb{T}^2$ .

**6.9. A combinatorial construction.** An explicit example of an almost self-similar basic family with an associated evolution that satisfies Assumptions 6.1 and 6.3 will be constructed in Section 8. Here we want to illustrate, somewhat informally, the “combinatorial properties” on which our construction is based. This illustration provides a graphical sketch of the procedure described in §6.2 on a specific example and substantiates the feasibility of our strategy of proof.

In this example, there are two basic moves, the action of which is depicted in Figure 5. The support of the functions  $\rho^1(0, \cdot)$  and  $\rho^2(0, \cdot)$  is contained in the grey “straight strip” and “bent strip” in the figure, respectively.

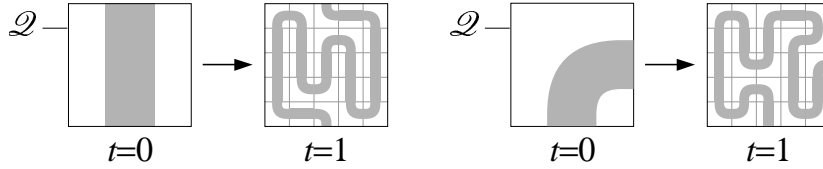


FIGURE 5. The two basic moves in the example of an almost self-similar construction. The solutions  $\rho^1$  (left) and  $\rho^2$  (right).

The two basic moves map  $\rho^1(0, \cdot) \rightsquigarrow \rho^1(1, \cdot)$  (Figure 5, left) and  $\rho^2(0, \cdot) \rightsquigarrow \rho^2(1, \cdot)$  (Figure 5, right), respectively. The output at time  $t = 1$  consists of configurations that (up to rotations) only include rescaled translations of functions with support contained in straight strips and in bent strips. This transition will be implemented with velocity fields that are supported in the same sets.

We remark that, in the actual construction, we take  $\lambda = 1/5$  and  $N = 6$ , since we have to consider the two rotations of the straight channel and the four rotations of the bent channel.

Figure 6 illustrates how we can patch these basic moves (following the procedure in §6.2) in order to obtain a velocity field and a solution that are compactly supported in  $\mathbb{R}^2$ . In detail, we implement the initial step in §6.2 with  $\bar{\lambda} = 1/2$  by starting at time  $t = 0$  with four bent channels that altogether create a “circular channel” (Figure 6, left). Each of the four bent channels then evolves according to the description in Figure 5: two steps in the evolution are illustrated in Figure 6. The resulting velocity field and solution are smooth and compactly supported, since we are able to control how the basic elements match at the interfaces between the four sub-squares.

The evolution in Figures 5 and 6 depicts the combinatorics of the example discussed in Section 8 accurately. However, the rigorous construction requires a careful analysis and implementation of these ideas, as we need to produce smooth solutions that are transported by smooth, divergence-free velocity fields.

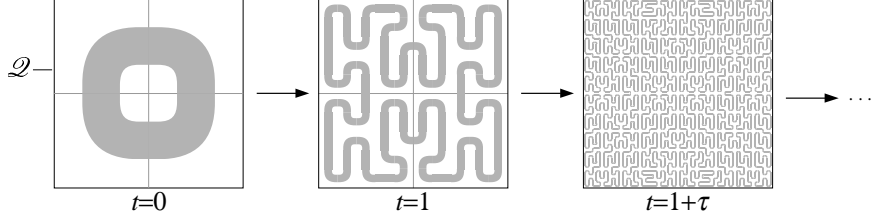


FIGURE 6. Patching of four basic moves and further steps in the almost self-similar evolution.

## 7. SECOND GEOMETRIC CONSTRUCTION

In this section we describe another geometric construction of divergence-free velocity fields  $u$  together with (non-trivial) solutions  $\rho$  of the continuity equation (1.1). For paths and curves we follow the notation introduced in Section 4. The main improvement in comparison to Section 4 is that we construct here solutions that are smooth.

We begin with a simple remark. Let  $I$  be a time interval and  $D$  an open subset of  $\mathbb{R}^2$ , and let  $\{\Phi(t, \cdot) : t \in I\}$  be an area-preserving flow on  $D$  of class  $C^k$  with  $k \geq 2$ , that is,  $\Phi : I \times D \rightarrow \mathbb{R}^2$  is a map of class  $C^k$  such that, for every  $t \in I$ ,  $\Phi(t, \cdot)$  is diffeomorphism from  $D$  into its image  $\Omega(t) := \Phi(t, D)$  which is area-preserving, which, for regular flows, is equivalent to imposing for every  $z \in D$ ,

$$J\Phi(t, z) := \det(\nabla \Phi(t, z)) = 1.$$

We denote by  $\Omega$  the (open) set of all points  $(t, x)$  with  $t \in I$  and  $x \in \Omega(t)$ . It is then well-known that the velocity field  $w : \Omega \rightarrow \mathbb{R}^2$  defined by

$$w(t, x) := \partial_t \Phi(t, z) \quad \text{with } x = \Phi(t, z) \quad (7.1)$$

is of class  $C^{k-1}$  and divergence-free.

Moreover, given a bounded function  $\bar{\rho}$  on  $D$ , the function  $\rho : I \times \Omega \rightarrow \mathbb{R}$  obtained by transporting  $\bar{\rho}$  with the flow  $\Phi$ , that is,  $\rho(t, x) := \bar{\rho}(z)$  when  $x = \Phi(t, z)$ , is a distributional solution of the continuity equation  $\partial_t \rho + \operatorname{div}(w\rho) = 0$  on  $\Omega$ .<sup>19</sup>

In the next proposition, we modify the previous construction in order to obtain a velocity field and a solution defined on  $I \times \mathbb{R}^2$ , rather than on  $I \times \Omega$ .

**Proposition 7.1.** *Let  $D$  and  $\Phi$  be as above with  $D$  a simply-connected domain, and let  $D'$  be a closed subset of  $D$ . Then, there exists a divergence-free velocity field  $u : I \times \mathbb{R}^2 \rightarrow \mathbb{R}^2$  of class  $C^{k-1}$  such that*

$$u(t, x) = w(t, x) = \partial_t \Phi(t, z), \quad \text{if } x = \Phi(t, z) \text{ for some } z \in D'. \quad (7.2)$$

<sup>19</sup> More precisely,  $\rho$  solves the transport equation  $\partial_t \rho + w \cdot \nabla \rho = 0$ , which agrees with the continuity equation  $\partial_t \rho + \operatorname{div}(w\rho) = 0$  because  $w$  is divergence-free.

Moreover, given a bounded function  $\bar{\rho} : D' \rightarrow \mathbb{R}$ , the function  $\rho : I \times \mathbb{R}^2 \rightarrow \mathbb{R}$  defined by

$$\rho(t, x) := \begin{cases} \bar{\rho}(z) & \text{if } x = \Phi(t, z) \text{ for some } z \in D', \\ 0 & \text{otherwise,} \end{cases} \quad (7.3)$$

is a distributional solution of the continuity equation (1.1).

*Remark 7.2.* The assumption that  $D$  is simply connected can be weakened, but not entirely removed.

Take indeed  $D := \mathbb{R}^2 \setminus \{0\}$  and let  $\{\Phi(t, \cdot) : t \geq 0\}$  be the flow on  $D$  associated with the (autonomous) velocity field  $w(x) := x/|x|^2$ . Since  $w$  is divergence-free on  $D$ , the flow is area-preserving. In addition, the flux of  $w$  through any closed curve  $\Gamma$  that winds around the origin once counterclockwise, is  $2\pi$ , since the distributional divergence of  $w$  on  $\mathbb{R}^2$  is  $2\pi \delta_0$ , with  $\delta_0$  the Dirac mass at the origin. On the other hand, the flux through  $\Gamma$  of any divergence-free velocity field  $u$  defined on  $\mathbb{R}^2$  must be 0. This fact means that (7.2) cannot hold for any set  $D'$  such that  $\Phi(t, D')$  contains such a curve  $\Gamma$  for some  $t$ .

**Proof of Proposition 7.1.** The main idea is simple. We pick  $w$  as in (7.1), and we let  $\phi$  be a potential of  $w$ . We then multiply this potential by a suitable cut-off function, which agrees with 1 on  $D'$ , and finally take as  $u$  the rotated gradient of the truncated potential, which ensures that  $u$  is divergence-free. We next present the proof in detail.

We choose a point  $z_0 \in D$  and smooth cut-off function  $g : \mathbb{R}^2 \rightarrow [0, 1]$  which agrees with 1 on a open neighbourhood of  $D'$  and has support contained in  $D$ . Since  $D$  is simply connected,  $\Omega(t)$  is simply connected for every  $t \in I$ , and consequently the divergence-free velocity field  $w(t, \cdot)$  admits a unique potential  $\phi(t, \cdot)$  in the sense of §4.11 that satisfies the normalization condition:

$$\phi(t, x_0(t)) = 0, \quad \text{where } x_0(t) := \Phi(t, z_0). \quad (7.4)$$

We then define the truncated potential  $\varphi(t, \cdot) : \mathbb{R}^2 \rightarrow \mathbb{R}$  by

$$\varphi(t, x) := \begin{cases} \phi(t, x) g(z) & \text{if } x = \Phi(t, z) \text{ for some } z \in D, \\ 0 & \text{otherwise,} \end{cases} \quad (7.5)$$

and finally take  $u := \nabla^\perp \varphi$ .

Since  $\Phi$  is of class  $C^k$ , both  $w$  and  $\phi$  are of class  $C^{k-1}$  in both variables, and  $\phi$  is of class  $C^k$  in  $x$ .<sup>20</sup> Clearly, the same holds for  $\varphi$ , which in turn implies that  $u$  is of class  $C^{k-1}$ . Moreover,  $\varphi$  agrees by construction with  $\phi$  on an open neighborhood  $U$  of the set of all points of the form  $\Phi(t, z)$  with  $t \in I$ ,  $z \in D'$ , and therefore  $u$  agrees with  $w$  on  $U$ ; in particular (7.2) holds.

Concerning the second part of the claim, we note that  $\rho$  is obtained by transporting  $\bar{\rho}$  with the flow  $\Phi$ , and hence it solves the continuity equation  $\partial_t \rho + \operatorname{div}(w\rho) = 0$  on  $\Omega$ . On the other hand,  $u$  and  $v$  agree on  $U$ , which contains

<sup>20</sup> Recall that  $\phi$  is given by the formula  $\phi(x) = \int_\Gamma w \cdot \eta \, d\sigma$  where  $\Gamma$  is any curve that starts from  $x_0(t)$  and ends at  $x$ .

the support of  $\rho$ , and therefore  $\rho$  solves the continuity equation  $\partial_t \rho + \operatorname{div}(u\rho) = 0$  as well.  $\square$

Let  $\Gamma$  be a curve in the plane. In the next lemma, we modify the definition of the parametrization  $\Psi$  of the tubular neighborhood  $B(\Gamma, r)$  given in (4.1), in order to obtain an area-preserving map.

**Lemma 7.3.** *Let  $\Gamma$  be a proper curve parametrized by a path  $\gamma : \mathbb{R} \rightarrow \mathbb{R}^2$  of class  $C^k$  with  $k \geq 3$ , such that  $|\dot{\gamma}(\cdot)| = \ell$  for some constant  $\ell$ . Let  $r$  be a positive number such that  $2r/\ell$  is smaller or equal than the tubular radius  $\bar{r}$  of  $\Gamma$ , assumed to be strictly positive, and let  $\Phi : \mathbb{R} \times (-r, r) \rightarrow \mathbb{R}^2$  be the map defined by*

$$\Phi(s, y) := \gamma(s) + \alpha(s, y/\ell) \eta(s) \quad \text{with} \quad \alpha(s, y') := \frac{2y'}{1 + \sqrt{1 - 2y'\kappa(s)}}. \quad (7.6)$$

*Then,  $\gamma(\cdot) = \Phi(\cdot, 0)$  and  $\Phi$  is an area-preserving diffeomorphism of class  $C^{k-2}$ , the image of which is contained in the tubular neighbourhood  $B(\Gamma, 2r/\ell)$  and contains  $B(\Gamma, r/(2\ell))$ .*

**Proof.** Using the assumption on  $r$  and the fact that the tubular radius  $\bar{r}$  is smaller or equal than the curvature radius  $1/|\kappa|$  of the curve, it follows that  $r \leq \ell/(2\kappa)$ , which implies that  $\Phi$  is well defined on  $\mathbb{R} \times (-r, r)$ .

We observe that  $\alpha$  is a function of class  $C^{k-2}$  because  $\kappa$  is of class  $C^{k-2}$ , and that

$$\Phi(s, y) = \Psi(s, \alpha(s, y/\ell)) \quad \text{for every } s, y, \quad (7.7)$$

where  $\Psi$  is defined in (4.1). Since  $\Psi$  is a diffeomorphism of class  $C^{k-1}$  on  $\mathbb{R} \times (-\bar{r}, \bar{r})$  and the function  $y \mapsto \alpha(s, y/\ell)$  has strictly positive derivative for every  $s$  and maps  $(-r, r)$  into  $(-\bar{r}, \bar{r})$ , we have that  $\Phi$  is a diffeomorphism of class  $C^{k-2}$ .

The fact that  $\Phi$  is area-preserving, that is,  $J\Phi = 1$  everywhere, can be verified by a direct computation. For this purpose, it is convenient to write the gradient of  $\Phi$  at  $(s, y)$  using the canonical basis of  $\mathbb{R}^2$  for the domain, and the orthonormal basis  $\tau(s), \eta(s)$  for the codomain, which gives

$$\nabla \Phi(s, y) = \begin{pmatrix} \ell(1 - \kappa \alpha) & 0 \\ \partial_s \alpha & \frac{1}{\ell} \partial_{y'} \alpha \end{pmatrix},$$

where  $\kappa = \kappa(s)$  and  $\alpha = \alpha(s, y/\ell)$ .

Finally, the fact that the image of  $\Phi$  is contained in  $B(\Gamma, 2r/\ell)$  and contains  $B(\Gamma, r/(2\ell))$  follows from formula (7.7) and the estimate  $1/(2\ell) \leq \alpha \leq 2/\ell$ .  $\square$

In the next subsections, we associate a velocity field  $u$  and a solution  $\rho$  of the continuity equation (1.1) to a given time-dependent proper curve  $\Gamma$ . This construction will provide the building blocks for the example described in the next section.

**7.4. Canonical velocity field associated to a time-dependent curve.** Let  $\Gamma$  be a time-dependent curve, parametrized by the path  $\gamma : I \times \mathbb{R} \rightarrow \mathbb{R}^2$  of class  $C^k$  with  $k \geq 3$ , and let  $r$  be a positive number such that

- (a)  $|\dot{\gamma}(t, \cdot)|$  is equal to some  $\ell(t) > 0$  for every  $t \in I$ ;
- (b)  $2r/\ell(t)$  is smaller or equal than the tubular radius of  $\Gamma(t)$  for every  $t \in I$ .

Now, for every  $t \in I$  we let  $\Phi(t, \cdot)$  be the diffeomorphism on  $D := \mathbb{R} \times (-r, r)$  defined by (7.6), and we take the velocity field  $u : I \times \mathbb{R}^2 \rightarrow \mathbb{R}^2$  as in Proposition 7.1, having set  $D' := \mathbb{R} \times [-r/2, r/2]$ .

A close inspection of the proof of Proposition 7.1 shows that the construction of  $u$  depends on the choice of the point  $z_0$  in  $\mathbb{R} \times (-r, r)$  used in the normalization condition (7.4), and the choice of the cut-off function  $g$ . For the construction at hand, we choose:<sup>21</sup>

- (c)  $z_0 := (0, 0)$ ,
- (d)  $g(s, y) := \bar{g}(y/r)$ , where  $\bar{g} : \mathbb{R} \rightarrow [0, 1]$  is a fixed smooth function that is *even*, takes value 1 in a neighbourhood of  $[-1/2, 1/2]$ , and its support is contained in  $(-1, 1)$ .

**7.5. Canonical solution associated to a time-dependent curve.** We fix an *even* bounded function  $\bar{\rho} : [-1/2, 1/2] \rightarrow \mathbb{R}$  with zero average and let  $\rho : I \times \mathbb{R}^2 \rightarrow \mathbb{R}$  be the solution of the continuity equation (1.1) obtained by replacing the function  $\bar{\rho}(z)$  in formula (7.3) with  $\bar{\rho}(y/r)$ , that is,

$$\rho(t, x) := \begin{cases} \bar{\rho}(y/r) & \text{if } x = \Phi(t, s, y) \text{ for some } s \in \mathbb{R}, y \in [-r/2, r/2], \\ 0 & \text{otherwise.} \end{cases} \quad (7.8)$$

*Remark 7.6.* (i) The velocity field  $u$  constructed above is uniquely determined by the choice of the parametrization  $\gamma$ , the number  $r$ , and the function  $\bar{g}$ . Since  $\bar{g}$  is fixed for the rest of the paper, the relevant parameters are therefore  $\gamma$  and  $r$ .

(ii) The solution  $\rho$  depends only on purely geometrical quantities, and not on the choice of the parametrization  $\gamma$ . More precisely, using formulas (7.6) and (7.8) one readily checks that the value  $\rho(t, x)$  is zero if  $\text{dist}(x, \Gamma(t)) > r/\ell(t)$ , and otherwise it depends on:

- $r$ ,  $t$ , and  $\ell(t)$ ;
- the distance  $\text{dist}(x, \Gamma(t))$ ;
- the curvature of  $\Gamma(t)$  at the projection of  $x$  on  $\Gamma(t)$ .

(iii) By construction, for every  $t \in I$ , the velocity field  $u(t, \cdot)$  is supported in  $\Phi(t, \mathbb{R} \times (-r, r))$ , which is contained in  $B(\Gamma(t), 2r/\ell(t))$ , while  $\rho(t, \cdot)$  is supported in  $\Phi(t, \mathbb{R} \times (-r/2, r/2))$ , which is contained in  $B(\Gamma(t), r/\ell(t))$  (cf. Lemma 7.3).

(iv) The requirement that  $\bar{\rho}$  has zero average and formula (7.8), together with the fact that the change of variable  $\Phi$  is area-preserving, imply that the solution  $\rho(t, \cdot)$  has zero average. This property will be used in Section 8.

<sup>21</sup> In the present context, the variable  $z$  agrees with  $(s, y)$ .

We suppose now that we are given two time-dependent curves  $\Gamma$  and  $\tilde{\Gamma}$ , and we let  $u, \tilde{u}$  and  $\rho, \tilde{\rho}$  be, respectively, the corresponding velocity fields and solutions constructed in §7.4 and §7.5. In the next section, we will need a sort of locality principle, informally stating that if  $\Gamma$  and  $\tilde{\Gamma}$  agree in a neighbourhood of some point  $x_0$ , then also  $u, \tilde{u}$  and  $\rho, \tilde{\rho}$  agree in a neighbourhood of  $x_0$ .

In Lemma 7.8 we give a precise statement of such a locality principle that is specifically designed for the application described in the next section. We first introduce some additional notation.

**7.7. Centered sub-arcs and curved rectangles.** Let  $\Gamma$  be a curve parametrized by a path  $\gamma$  such that  $|\dot{\gamma}(\cdot)| = \ell$  constant, and let  $x_0 = \gamma(s_0)$  be a point on  $\Gamma$ . For a given  $\delta > 0$ , we denote by  $I(\Gamma, x_0, \delta)$  the (centered) sub-arc of all  $x \in \Gamma$  such that their geodesic distance from  $x_0$  is strictly less than  $\delta$ , that is,

$$I(\Gamma, x_0, \delta) := \gamma((s_0 - \delta/\ell, s_0 + \delta/\ell)).$$

Moreover, given a  $\delta' > 0$  that is smaller or equal than the tubular radius of  $\Gamma$ , we denote by  $R(\Gamma, x_0, \delta, \delta')$  the (open, centered) curved rectangle of all  $x \in \mathbb{R}^2$  such that their distance from  $\Gamma$  is strictly less than  $\delta'$  and such that their projection on  $\Gamma$  belongs to  $I(\Gamma, x_0, \delta)$ , that is

$$R(\Gamma, x_0, \delta, \delta') := \Psi((s_0 - \delta/\ell, s_0 + \delta/\ell) \times (-\delta', \delta')),$$

where  $\Psi$  is given in (4.1).

**Lemma 7.8.** *Let  $\Gamma$  and  $\tilde{\Gamma}$  be two time-dependent, proper curves of class  $C^3$ , parametrized by  $\gamma, \tilde{\gamma} : I \times \mathbb{R} \rightarrow \mathbb{R}^2$  respectively. Assume that conditions (a) and (b) in §7.4 are verified by  $\gamma$  and  $\tilde{\gamma}$  with the same  $\ell : I \rightarrow (0, +\infty)$  and the same  $r > 0$ . Let then  $u, \tilde{u}$  be defined as in §7.4 and  $\rho, \tilde{\rho}$  be defined as in §7.5.*

*Assume, in addition, that there exist  $\delta > 0$  and  $s_0 \in \mathbb{R}$  such that for every  $t \in I$ ,*

- (a)  $\gamma(t, s_0) = \tilde{\gamma}(t, 0) =: x_0(t)$ ;
- (b) *the sub-arcs  $I(\Gamma(t), x_0(t), \delta)$  and  $I(\tilde{\Gamma}(t), x_0(t), \delta)$  coincide and have the same orientation;*
- (c) *the following condition is satisfied:*

$$\int_{\gamma(t, [0, s_0])} v_n(t, x) d\sigma(x) = 0,$$

*where  $v_n$  denotes the normal velocity of  $\Gamma$ ,*

*Then,  $u(t, x) = \tilde{u}(t, x)$  and  $\rho(t, x) = \tilde{\rho}(t, x)$  for every  $t \in I$  and every  $x$  in the curved rectangle  $R(t) := R(\Gamma(t), x_0(t), \delta, 2r/\ell(t))$ .*

**Proof.** The proof is not difficult, but we must revisit the entire construction of  $u$  and  $\rho$ , which is divided between §7.4, §7.5, and the proofs of Proposition 7.1 and Lemma 7.3.

We shall fix  $t \in I$ . Using assumptions (a) and (b), and the fact that  $\gamma(t, \cdot)$  and  $\tilde{\gamma}(t, \cdot)$  have the same parametrization speed  $\ell(t)$ , we obtain that

$$\gamma(t, s + s_0) = \tilde{\gamma}(t, s) \quad \text{when } |s| \leq \delta/\ell.$$



From this identity, it readily follows that the flows  $\Phi$  and  $\tilde{\Phi}$  defined by (7.6) satisfy

$$\Phi(t, s + s_0, y) = \tilde{\Phi}(t, s, y) \quad \text{when } |s| \leq \delta/\ell, |y| < r, \quad (7.9)$$

which implies that the velocity fields  $w$  and  $\tilde{w}$  defined by (7.1) satisfy

$$w(t, x) = \tilde{w}(t, x) \quad \text{when } x \in U(t), \quad (7.10)$$

where

$$U(t) := \{ \tilde{\Phi}(t, s, y) : |s| \leq \delta/\ell, |y| < r \}.$$

Let now  $\phi(t, \cdot)$  and  $\tilde{\phi}(t, \cdot)$  be the potentials of  $w(t, \cdot)$  and  $\tilde{w}(t, \cdot)$ , respectively, constructed in the proof of Proposition 7.1. We claim that

$$\phi(t, x) = \tilde{\phi}(t, x) \quad \text{when } x \in U(t). \quad (7.11)$$

Since the corresponding fields agree on  $U$ , it suffices to show that these potentials agree at one point of  $U$ , and we can actually show that they both vanish at  $x_0(t)$ . Indeed, formula (7.4), statement (c) in §7.4, and the identities  $\Phi(t, 0, 0) = \gamma(t, 0)$  and  $\tilde{\Phi}(t, 0, 0) = \tilde{\gamma}(t, 0)$  yield

$$\phi(t, \gamma(t, 0)) = \tilde{\phi}(t, \tilde{\gamma}(t, 0)) = 0.$$

Next, as  $\tilde{\gamma}(t, 0) = x_0(t)$ , we obtain

$$\tilde{\phi}(t, x_0(t)) = 0.$$

Finally, since  $x_0(t) = \gamma(t, s_0)$ , taking into account assumption (c) and the identity  $v_n = w \cdot \eta$ , it follows that

$$\begin{aligned} \phi(t, x_0(t)) &= \phi(t, \gamma(t, s_0)) = \phi(t, \gamma(t, s_0)) - \phi(t, \gamma(t, 0)) \\ &= \int_{\gamma(t, [0, s_0])} w \cdot \eta \, d\sigma = \int_{\gamma(t, [0, s_0])} v_n \, d\sigma = 0, \end{aligned}$$

and the proof of (7.11) is complete.

The rest of the proof is straightforward: from (7.11) and the choice of the cut-off function  $g$  (see requirement (d) in §7.4) we obtain that the truncated potentials  $\varphi(t, \cdot)$  and  $\tilde{\varphi}(t, \cdot)$  defined by (7.5) agree on  $U(t)$ . Moreover, one can show that both potentials vanish on  $R(t) \setminus U(t)$ , and therefore they agree on the whole  $R(t)$ , which implies that the corresponding velocity fields  $u(t, \cdot)$  and  $\tilde{u}(t, \cdot)$  agree on  $R(t)$ .

It remains to show that

$$\rho(t, x) = \tilde{\rho}(t, x) \quad \text{when } x \in R(t), \quad (7.12)$$

but this fact follows from Remark 7.6(ii).  $\square$

## 8. SECOND EXAMPLE: PEANO SNAKE

In this final section we verify Assumptions 6.1 and 6.3 for any  $s$  and  $p$  for the specific example, already illustrated in §6.9. By doing this, we validate the assumptions of Theorem 6.7; in particular, we establish the existence of a bounded, divergence-free velocity field supported in the unit square, which is Lipschitz uniformly in time, and the existence of a solution of the continuity equation (1.1), the functional and geometric mixing scales of which decay exponentially in time. We call this example the “Peano snake”, since the construction is reminiscent of the iterative construction of the Peano curve.

The velocity field and the solution provided by our construction are, in fact, smooth in both time and space (see Remark 8.9). However, any Sobolev norm of order higher than one is not uniformly bounded in time.

We proceed as follows. Using the tools provided in Section 7, we prove in §8.5, §8.6, and §8.7 that verifying the validity of Assumptions 6.1 and 6.3 can be reduced to showing the existence of two time-dependent, proper curves satisfying a certain number of geometric conditions described in §8.1 and §8.3. In §8.10, §8.11, and §8.12, we finally show how the two curves are actually constructed.

**8.1. Quasi self-similar basic curves: conditions.** The fundamental ingredients of our construction will be two time-dependent proper curves  $\Gamma_1(t)$  and  $\Gamma_2(t)$ , with parametrizations  $\gamma_1(t, s), \gamma_2(t, s) : [0, 1] \times \mathbb{R} \rightarrow \mathbb{R}^2$  of class  $C^\infty$ , such that, for every  $t \in [0, 1]$ :

- (a)  $\gamma_1(t, 0) = \gamma_2(t, 0) = (0, -1/2)$ ,  $\gamma_1(t, 1) = (0, 1/2)$ , and  $\gamma_2(t, 1) = (1/2, 0)$ ;
- (b) there exists a constant  $\delta > 0$  such that outside the square  $(1 - \delta)\mathcal{Q}$ , homothetic to  $\mathcal{Q}$ , each of the curves  $\Gamma_1(t)$  and  $\Gamma_2(t)$  agrees with two unbounded half-lines, orthogonal to  $\partial\mathcal{Q}$  through the points defined in (a);
- (c)  $|\dot{\gamma}_1(t, s)| = |\dot{\gamma}_2(t, s)| =: \ell(t)$ , and in particular the intersections of the curves  $\Gamma_1(t)$  and  $\Gamma_2(t)$  with  $\mathcal{Q}$  have length  $\ell(t)$  for every  $t$ ;
- (d) denoting by  $v_n^1$ , resp.  $v_n^2$ , the normal velocity of  $\Gamma_1$ , resp.  $\Gamma_2$ ,

$$\int_{\gamma_1(t, [0, 1])} v_n^1(t, x) d\sigma(x) = 0, \quad \text{resp.} \quad \int_{\gamma_2(t, [0, 1])} v_n^2(t, x) d\sigma(x) = 0;$$

- (e) for every square  $Q$  that agrees with one the 25 squares in the tiling  $\mathcal{T}_{1/5}$  of  $\mathcal{Q}$ , the sub-arc  $\Gamma_1(1) \cap Q$  can be written as a translated, rescaled, and possibly rotated copy of  $\Gamma_1(0) \cap \mathcal{Q}$  or  $\Gamma_2(0) \cap \mathcal{Q}$ ; the same holds for  $\Gamma_2(1) \cap Q$ .

**8.2. Explanation of the combinatorics.** An example of curves satisfying (some of) the conditions in §8.1 is illustrated in Figure 7. In this figure, we can see the evolution of  $\Gamma_1$  starting from a straight segment  $\Gamma_1(0)$  inside  $\mathcal{Q}$ , and the evolution of  $\Gamma_2$  starting from a (slightly modified) quarter of circle  $\Gamma_2(0)$  inside  $\mathcal{Q}$ . Both  $\Gamma_1(1)$  and  $\Gamma_2(1)$  consist of (rescaled, translated, and rotated) straight segments and (slightly modified) quarters of circles.

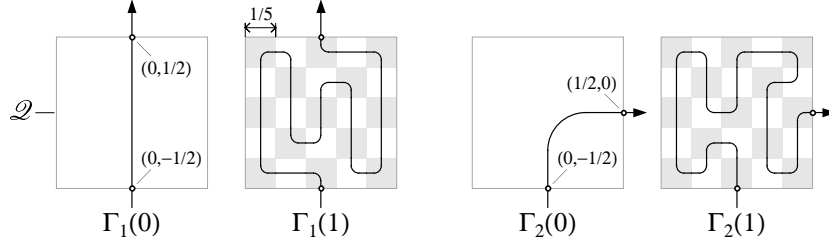


FIGURE 7. Toy example of basic curves satisfying (a), (b), and (e) in §8.1.

From the geometry of  $\Gamma_1$  and  $\Gamma_2$  as depicted in Figure 7, it follows that the curves satisfy conditions (a), (b), and (e) (which is the most relevant), while they do not satisfy condition (c), and condition (d) depends on the parametrization and cannot be verified from the picture. In fact, providing examples of basic curves satisfying all the assumptions in §8.1 is significantly more complex and the construction will be carried out in §8.10, §8.11, and §8.12.

The combinatorial structure of our construction has been explained in §6.9. As illustrated in Figure 8, we patch together four (rotated) copies of the curve  $\Gamma_2(0)$  and we let each of them evolve as described in Figure 7. The “matching” of the curves at the interfaces between the four sub-squares will be essential in establishing the smoothness of the velocity field and the solutions, which is done in §8.7 and §8.8.

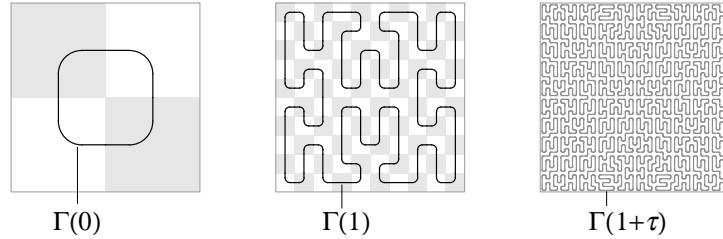


FIGURE 8. Patching together four copies of  $\Gamma_2$ , and subsequent evolution in time.

**8.3. Reduction: simplified geometric conditions.** We shall consider the following alternative assumptions (c'), (c''), and (d'), in which we denote by  $\ell_1(t)$ , resp.  $\ell_2(t)$ , the length of the intersection of the curve  $\Gamma_1(t)$ , resp.  $\Gamma_2(t)$ , with  $\mathcal{Q}$ :

- (c')  $\ell_1(0) = \ell_2(0)$ ;
- (c'') the derivatives in  $t$  of the functions  $\ell_1(t)$  and  $\ell_2(t)$  are strictly positive;
- (d') the area of each of the two connected components of  $\mathcal{Q} \setminus \Gamma_1(t)$  equals  $1/2$ , and the same holds for the area of the two connected components of  $\mathcal{Q} \setminus \Gamma_2(t)$ .

We claim that assumptions (b)–(c′)–(c′′)–(d′)–(e) imply the full set of assumptions (a)–(b)–(c)–(d)–(e) in §8.1. First of all, (a) follows from (b) by choosing suitable parametrizations  $\gamma_1(t, \cdot)$  and  $\gamma_2(t, \cdot)$ . Next, we can modify such parametrizations in such a way that  $|\dot{\gamma}_1(t, \cdot)|$  and  $|\dot{\gamma}_2(t, \cdot)|$  are constant for all  $t$ . This fact, together with (a), entails that  $|\dot{\gamma}_1(t, s)| = \ell_1(t)$  and  $|\dot{\gamma}_2(t, s)| = \ell_2(t)$ . Assumption (c′), together with assumption (e), implies that  $\ell_1(1) = \ell_2(1) = 5\ell_1(0)$ . Then, assumption (c′′) implies that with a change of variable in  $t$  we can achieve  $\ell_1(t) = \ell_2(t) =: \ell(t)$  for all  $t$ , that is, assumption (c) holds. Finally, recalling Remark 4.7(iii), we have that (d) and (d′) are equivalent.

*Remark 8.4.* We will construct in §8.10, §8.11, and §8.12 at the end of this section two curves  $\Gamma_1$  and  $\Gamma_2$  that do satisfy the set of conditions in §8.3. The advantage is that the conditions in §8.3 are purely geometrical, in the sense that they are written in terms of the curves  $\Gamma_1$  and  $\Gamma_2$ , and do not involve the parametrizations  $\gamma_1$  and  $\gamma_2$ , which therefore will not be described.

In the next subsections, we assume the existence of two quasi self-similar basic curves as in §8.1 that we then patch together as in §8.2. We use the results in Section 7 to construct the associated velocity fields and solutions, and then prove they satisfy Assumptions 6.1 and 6.3. Finally, we establish additional regularity properties of these velocity fields and solutions.

**8.5. Construction of velocity fields and solutions.** Given the two time-dependent proper curves  $\Gamma_1$  and  $\Gamma_2$  as in §8.1, we choose a small  $r > 0$  such that:

- $r < \min\{r_1(t)\ell(t)/2, r_2(t)\ell(t)/2\}$  for every  $t \in [0, 1]$ , where  $r_1(t)$ , resp.  $r_2(t)$ , is the tubular radius of  $\Gamma_1(t)$ , resp. of  $\Gamma_2(t)$ , and  $\ell(t)$  is as in §8.1(c);
- $B(\Gamma_1(t), 2r) \subset \mathcal{Q}$  and  $B(\Gamma_2(t), 2r) \subset \mathcal{Q}$  for every  $t \in [0, 1]$ .

Such an  $r$  exists due to the smoothness of  $\Gamma_1$  and  $\Gamma_2$ , and assumption (b) in §8.1.

Then, we apply the constructions in §7.4 and §7.5 to construct two associated time-dependent divergence-free velocity fields  $u_1$  and  $u_2$  of class  $C^\infty$ , and two associated solutions  $\rho_1$  and  $\rho_2$  of class  $C^\infty$  of the continuity equation (1.1). One readily checks that:

- (a)  $u_1(t, \cdot)$  and  $\rho_1(t, \cdot)$  are supported in  $B(\Gamma_1(t), 2r/\ell(t))$ , while  $u_2(t, \cdot)$  and  $\rho_2(t, \cdot)$  are supported in  $B(\Gamma_2(t), 2r/\ell(t))$ ;
- (b)  $u_1(t, \cdot)$  and  $\rho_1(t, \cdot)$  vanish on  $\partial\mathcal{Q} \setminus ((\frac{-2r}{\ell(t)}, \frac{2r}{\ell(t)}) \times \{\frac{-1}{2}\} \cup (\frac{-2r}{\ell(t)}, \frac{2r}{\ell(t)}) \times \{\frac{1}{2}\})$ , while  $u_2(t, \cdot)$  and  $\rho_2(t, \cdot)$  vanish on  $\partial\mathcal{Q} \setminus ((\frac{-2r}{\ell(t)}, \frac{2r}{\ell(t)}) \times \{\frac{-1}{2}\} \cup \{\frac{1}{2}\} \times (\frac{-2r}{\ell(t)}, \frac{2r}{\ell(t)}))$ ;
- (c)  $u_1(t, \cdot)$  and  $u_2(t, \cdot)$  are tangent to the boundary  $\partial\mathcal{Q}$ .

Indeed, (a) and (b) follow at once from Remark 7.6(iii).

Let us prove (c) for the curve  $\Gamma_1$ , the proof for  $\Gamma_2$  being analogous. Consider the vertical line  $\tilde{\Gamma}(t)$  with parametrization  $\tilde{\gamma}(t, s) = (0, \frac{1}{2} + s\ell(t))$  and let  $\tilde{u}$  be the velocity field associated to  $\tilde{\Gamma}$  as in §7.4. We use Lemma 7.8 with  $s_0 = 1$  and  $x_0(t) = (0, \frac{1}{2})$ . We observe that assumption (b) of the lemma is satisfied with

the same  $\delta > 0$  as in condition (b) in §8.1, while assumption (c) follows from condition (d) in §8.1; all other assumptions of the lemma are clearly satisfied by our choice of  $\tilde{\Gamma}$ .

Lemma 7.8 then implies that for any  $t \in [0, 1]$ , the velocity field  $\tilde{u}(t, \cdot)$  coincides with  $u_1(t, \cdot)$  in the curved rectangle  $R(\Gamma_1(t), (0, \frac{1}{2}), \delta, \frac{2r}{\ell(t)})$ , which in this case coincides with the rectangle  $(\frac{-2r}{\ell(t)}, \frac{2r}{\ell(t)}) \times (\frac{1}{2} - \delta, \frac{1}{2} + \delta)$ .

It is, therefore, sufficient to show that  $\tilde{u}(t, \cdot)$  is tangent to  $(\frac{-2r}{\ell(t)}, \frac{2r}{\ell(t)}) \times \{\frac{1}{2}\}$  for any  $t \in [0, 1]$ . This property follows from the fact that the area-preserving diffeomorphism  $\tilde{\Phi}$  in (7.6) associated to  $\tilde{\Gamma}$  has the form

$$\tilde{\Phi}(t, y) = \left( \frac{y}{\ell(t)}, \frac{1}{2} + s\ell(t) \right),$$

and from the construction in §7.4.

The fact that  $u_1(t, \cdot)$  is tangent to  $(\frac{-2r}{\ell(t)}, \frac{2r}{\ell(t)}) \times \{\frac{1}{2}\}$  can be proved in an analogous manner, by considering the line  $\tilde{\Gamma}$  parametrized by  $\tilde{\gamma}(t, s) = (0, -\frac{1}{2} + s\ell(t))$ ,  $s_0 = 0$ , and  $x_0(t) = (0, -\frac{1}{2})$ .

**8.6. Verification of Assumption 6.1.** First, we recall that the velocity fields  $u_1$  and  $u_2$  are smooth, and in particular satisfy Assumption 6.1(i), while Assumption 6.1(ii) follows from Remark 7.6(iv). Assumption 6.1(iii) can be obtained combining the fact that the solutions  $\rho_1$  and  $\rho_2$  can be described in purely geometric terms (Remark 7.6(ii)) and the quasi self-similarity of the curves  $\Gamma_1$  and  $\Gamma_2$  in condition (e) in §8.1.

**8.7. Verification of Assumption 6.3.** According to the general scheme for a quasi self-similar construction (§6.2), and to the specific combinatorial structure of our example (§8.2), we have that, for times  $T_n < t \leq T_{n+1}$ , on each square of the tiling  $\mathcal{T}_{1/(2 \cdot 5^n)}$  the velocity field  $u$  equals a rotated and rescaled translation of one of the velocity fields associated (according to the procedure in §8.5) to the curves  $\Gamma_1$  and  $\Gamma_2$  in §8.1.

We check that  $u$  is in fact smooth on the entire  $\mathbb{R}^2$ . This fact implies Assumption 6.3 for any  $s$  and  $p$ . The regularity in the interior of each square of the tiling  $\mathcal{T}_{1/(2 \cdot 5^n)}$  follows from the regularity of  $u_1$  and  $u_2$  (§8.5). We are therefore left with checking the regularity across the boundary of  $\mathcal{Q}$ , and at the interface between each pair of squares of the tiling.

The combinatorial structure in §8.2 guarantees that, at every time, the rotated and rescaled translations of the curves  $\Gamma_1$  and  $\Gamma_2$  never intersect the boundary of  $\mathcal{Q}$ : they intersect the boundary of squares of the tiling always at the interface with another square of the tiling, and never at the boundary of  $\mathcal{Q}$ . Together with §8.5(b), this observation implies that the velocity field  $u$  vanishes in a neighborhood of the boundary of  $\mathcal{Q}$ , which ensures the regularity across the boundary of  $\mathcal{Q}$ .

The proof of the regularity at the interface between each pair of squares of the tiling is based on Lemma 7.8. We fix  $Q' \in \mathcal{T}_{1/(2 \cdot 5^n)}$  and call  $\Gamma'$  the rotated

and rescaled translation of one of the curves  $\Gamma_1$  and  $\Gamma_2$ , which lies inside  $Q'$  (see Figure 9). We next fix one of the sides of  $Q'$  that is intersected by  $\Gamma'$  at its middle point and call it  $\Sigma$ . We call  $Q'' \in \mathcal{T}_{1/(2 \cdot 5^n)}$  the square which lies immediately across  $\Sigma$ , and call  $\Gamma''$  the rotated and rescaled translation of one of the curves  $\Gamma_1$  and  $\Gamma_2$  which lies inside  $Q''$ . Then, the combinatorial structure in §8.2 guarantees that also  $\Gamma''$  intersects  $\Sigma$  at its middle point.

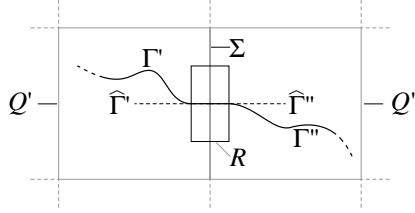


FIGURE 9. The situation in §8.7.

We now recall (see §6.2 and §8.1(b)) that the curve  $\Gamma'$ , resp.  $\Gamma''$ , has been defined as the intersection with  $Q'$ , resp.  $Q''$ , of the curve  $\hat{\Gamma}'$ , resp.  $\hat{\Gamma}''$ , which agrees with an half-line outside of  $(1 - \delta/(2 \cdot 5^n))Q'$ , resp.  $(1 - \delta/(2 \cdot 5^n))Q''$ . Consequently, there is a rectangle  $R$  of height  $\delta/5^n$  centered at the middle point of  $\Sigma$  such that  $\hat{\Gamma}'$  and  $\hat{\Gamma}''$  coincide inside  $R$  with a straight line orthogonal to  $\Sigma$ .

We can, therefore, argue as in the proof of item (c) in §8.5 and prove that the velocity fields  $\hat{u}'$  and  $\hat{u}''$  generated by  $\hat{\Gamma}'$  and  $\hat{\Gamma}''$  coincide inside  $R$ . Since both  $\hat{u}'$  and  $\hat{u}''$  are smooth, it is then clear that the restriction of  $\hat{u}'$  to  $Q'$  patched with the restriction of  $\hat{u}''$  to  $Q''$  is smooth, given that the velocity fields are tangent to the boundary of the squares.

We have therefore checked Assumption 6.3.

**8.8. Regularity in space of solutions.** The same procedure in §8.7 can be applied to the solution  $\rho$ , which is therefore smooth in the whole  $\mathbb{R}^2$  for every time  $t$ .

**8.9. Regularity in time of velocity fields and solutions.** In §8.7 and §8.8, we have proved that the velocity fields and the solutions are smooth with respect to the space. In fact, they are also smooth with respect to the time for  $0 \leq t \leq 1$ : this property follows from the smoothness with respect to the time of the basic curves in §8.1.

We can apply the procedure described in §3.6 and obtain velocity fields and solutions that are smooth with respect to both space and time, for  $x \in \mathbb{R}^2$  and  $t \geq 0$ . We stress that we are *not* asserting that Sobolev norms of order higher than one are bounded *uniformly in time*: in fact, they blow up exponentially in time (see Remark 6.8(iii)). This construction will be relevant for the companion paper [3], which addresses the issue of the instantaneous loss of fractional regularity of solutions of the continuity equation (1.1).

As announced before, we conclude this section by constructing two time-dependent curves  $\Gamma_1, \Gamma_2$  on the time interval  $I = [0, 1]$  that satisfy assumptions (b), (c'), (c''), (d') and (e) in §8.3.

Due to the complexity that a rigorous construction would entail, we only give a precise description of the initial states  $\Gamma_1(0), \Gamma_2(0)$ , and of the final states  $\Gamma_1(1), \Gamma_2(1)$  (see Figure 10) and sketch some of the intermediate states (Figures 11 and 13).

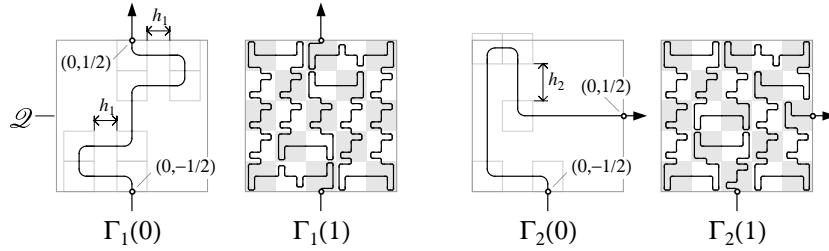


FIGURE 10. The curves  $\Gamma_1$  and  $\Gamma_2$  for  $t = 0$  and  $t = 1$ .

**8.10. Construction of  $\Gamma_1$  and  $\Gamma_2$  for  $t = 0, t = 1$ .** We take  $\Gamma_1$  and  $\Gamma_2$  at the initial time  $t = 0$  and at the final time  $t = 1$  as in Figure 10. Note that the curves  $\Gamma_1(0)$  and  $\Gamma_2(0)$  have been obtained by modifying the curves described in Figure 7 (which do not satisfy requirements (c') and (d') in §8.3). We specify that:

- all the small squares drawn in the first and third picture in Figure 10 have sidelength  $1/5$ ;
- outside these small squares the curves  $\Gamma_1(0)$  and  $\Gamma_2(0)$  consists of segments and half-lines;
- the intersections of  $\Gamma_1(0)$  and  $\Gamma_2(0)$  with the small squares are not exactly quarters of circle, but smooth curves chosen in such a way that  $\Gamma_1(0)$  and  $\Gamma_2(0)$  are smooth; these modified quarters of circle agree up to reflections, rotations, and translations;
- the construction parameter  $h_1$  and  $h_2$  are chosen so that  $\Gamma_1(0)$  and  $\Gamma_2(0)$  satisfy requirements (c') and (d'): we first choose  $h_2$  so that  $\Gamma_2(0)$  satisfies the equal-area requirement (d') (note that  $\Gamma_1(0)$  satisfies (d') independently of the choice of  $h_1$  for symmetry reasons), and then we choose  $h_1$  so that  $\Gamma_1(0)$  and  $\Gamma_2(0)$  have the same length in  $\mathcal{Q}$ , that is, (c') holds;
- finally, both  $\Gamma_1(1)$  and  $\Gamma_2(1)$  consist of 25 copies of  $\Gamma_1(0)$  and  $\Gamma_2(0)$ , rotated, reflected, translated, and scaled by a factor  $1/5$ ; thus requirement (e) is met.

**8.11. Construction of  $\Gamma_1(t)$  for  $0 < t < 1$ .** The transition from  $\Gamma_1(0)$  to  $\Gamma_1(1)$  is given in Figure 11. More precisely, we specify that:

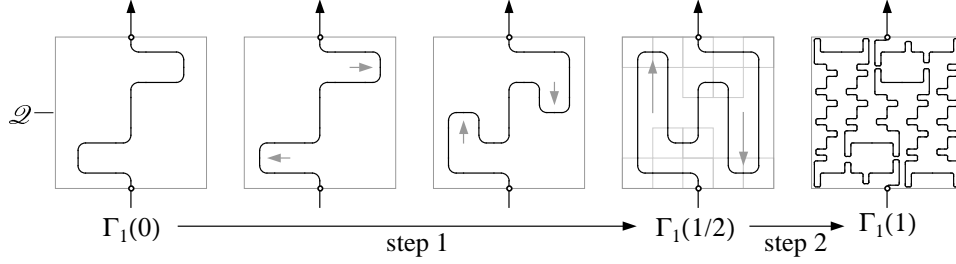


FIGURE 11. The evolution of  $\Gamma_1$  from  $t = 0$  to  $t = 1$  in two steps.



FIGURE 12. Details of the moves used in the second step of the evolution of  $\Gamma_1$ .

- the small squares drawn in the fourth picture have sidelength  $1/5$ , and within each of these squares,  $\Gamma_1(1/2)$  agrees with one of the modified quarters of circle used in §8.10;
- in the second step, we modify  $\Gamma_1(1/2)$  within each square of  $\mathcal{T}_{1/5}$  using one of “moves” described in Figure 12;
- it is clear that  $\Gamma_1$  satisfies requirement (c’), that is,  $\ell_1(t)$  is increasing in  $t$  for  $0 \leq t \leq 1$ ;
- $\Gamma_1$  satisfies the equal-area requirement (d’) during the first step because of the symmetry of the evolution;
- $\Gamma_1$  satisfies the equal-area requirement (d’) also during the second step: we remark indeed that every move of the first type in Figure 12 preserves the equal-area condition, while the moves of the second type can be coupled so that to each move that increases the area of one connected component of  $\mathcal{Q} \setminus \Gamma_1(t)$  (in some square of  $\mathcal{T}_{1/5}$ ) corresponds a move that decreases the area of that component (in another square).

**8.12. Construction of  $\Gamma_2(t)$  for  $0 < t < 1$ .** The transition from  $\Gamma_2(0)$  to  $\Gamma_2(1)$  is described in Figure 13. More precisely, we specify that:

- the small squares drawn in the third picture have sidelength  $1/5$ , and within each of these squares  $\Gamma_2(1/4)$  agrees with one of the modified quarters of circle used in §8.10;
- it is clear that requirement (c’’) is satisfied during the entire evolution;
- the equal-area requirement (d’) is satisfied during the first step of this evolution for reasons of symmetry;



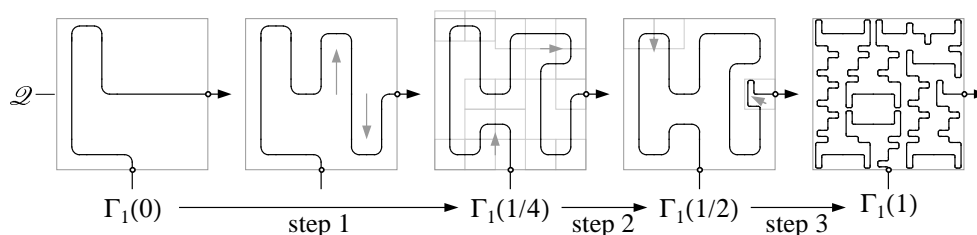


FIGURE 13. The evolution of  $\Gamma_2$  from  $t = 0$  to  $t = 1$  in three steps.

- most of  $\Gamma_2$  is kept fixed by the evolution in the second step, except the part contained in the two squares on top-left corner of  $\mathcal{Q}$ , which moves downward, and the part contained in the middle square of the right side, which evolves according to the second move in Figure 12; the equal-area requirement (d') is satisfied at time  $t = 1/2$ , and is satisfied also for the intermediate times  $1/4 < t < 1/2$  provided that these two moves are suitably “synchronized”, by a change of time for one of the two basic moves;
- in the third step we modify  $\Gamma_2(1/2)$  within each square in  $\mathcal{T}_{1/5}$  (except the middle square on in the right side of  $\mathcal{Q}$ ) using one of the moves described in Figure 12; note that this step satisfies the equal-area requirement (d') for the same reasons as the last step of the evolution of  $\Gamma_1$  does.

## REFERENCES

- [1] G. Alberti, S. Bianchini, and G. Crippa. Structure of level sets and Sard-type properties of Lipschitz maps. *Ann. Sc. Norm. Super. Pisa Cl. Sci. (5)*, 12(4):863–902, 2013.
- [2] G. Alberti, S. Bianchini, and G. Crippa. A uniqueness result for the continuity equation in two dimensions. *J. Eur. Math. Soc. (JEMS)*, 16(2):201–234, 2014.
- [3] G. Alberti, G. Crippa, and A. L. Mazzucato. Loss of regularity for continuity equations with non-Lipschitz velocity. Paper in preparation.
- [4] G. Alberti, G. Crippa, and A. L. Mazzucato. Exponential self-similar mixing and loss of regularity for continuity equations. *C. R. Math. Acad. Sci. Paris*, 352(11):901–906, 2014.
- [5] L. Ambrosio. Transport equation and Cauchy problem for BV vector fields. *Invent. Math.*, 158(2):227–260, 2004.
- [6] L. Ambrosio and G. Crippa. Continuity equations and ODE flows with non-smooth velocity. *Proc. Roy. Soc. Edinburgh Sect. A*, 144(6):1191–1244, 2014.
- [7] H. Aref. Stirring by chaotic advection. *J. Fluid Mech.*, 143:1–21, 1984.
- [8] H. Bahouri, J.-Y. Chemin, and R. Danchin. *Fourier analysis and nonlinear partial differential equations*. Grundlehren der Mathematischen Wissenschaften, 343. Springer-Verlag, Berlin-Heidelberg, 2011.
- [9] J. Bedrossian, N. Masmoudi, and V. Vicol. Enhanced dissipation and inviscid damping in the inviscid limit of the Navier-Stokes equations near the two dimensional Couette flow. *Arch. Ration. Mech. Anal.*, 219(3):1087–1159, 2016.
- [10] J. Bergh and J. Löfström. *Interpolation spaces. An introduction*. Grundlehren der Mathematischen Wissenschaften, 223. Springer-Verlag, Berlin-Heidelberg, 1976.

- [11] G. Boffetta, A. Celani, M. Cencini, G. Lacorata, and A. Vulpiani. Nonasymptotic properties of transport and mixing. *Chaos*, 10(1):50–60, 2000.
- [12] F. Bouchut and G. Crippa. Lagrangian flows for vector fields with gradient given by a singular integral. *J. Hyperbolic Differ. Equ.*, 10(2):235–282, 2013.
- [13] A. Bressan. A lemma and a conjecture on the cost of rearrangements. *Rend. Sem. Mat. Univ. Padova*, 110:97–102, 2003.
- [14] F. Colombini, T. Luo, and J. Rauch. Nearly Lipschitzian divergence-free transport propagates neither continuity nor BV regularity. *Commun. Math. Sci.*, 2(2):207–212, 2004.
- [15] P. Constantin, A. Kiselev, L. Ryzhik, and A. Zlatoš. Diffusion and mixing in fluid flow. *Ann. of Math. (2)*, 168(2):643–674, 2008.
- [16] G. Crippa and C. De Lellis. Estimates and regularity results for the DiPerna-Lions flow. *J. Reine Angew. Math.*, 616:15–46, 2008.
- [17] G. Crippa and C. Schulze. Paper in preparation.
- [18] N. Depauw. Non unicité des solutions bornées pour un champ de vecteurs BV en dehors d’un hyperplan. *C. R. Math. Acad. Sci. Paris*, 337(4):249–252, 2003.
- [19] E. Di Nezza, G. Palatucci, and E. Valdinoci. Hitchhiker’s guide to the fractional Sobolev spaces. *Bull. Sci. Math.*, 136(5):521–573, 2012.
- [20] R. J. DiPerna and P.-L. Lions. Ordinary differential equations, transport theory and Sobolev spaces. *Invent. Math.*, 98(3):511–547, 1989.
- [21] D. P. G. Foures, C. P. Caulfield, and P. J. Schmid. Optimal mixing in two-dimensional plane Poiseuille flow at finite Péclet number. *J. Fluid Mech.*, 748:241–277, 2014.
- [22] T. Gotoh and T. Watanabe. Scalar flux in a uniform mean scalar gradient in homogeneous isotropic steady turbulence. *Phys. D*, 241(3):141–148, 2012.
- [23] E. Gouillart, O. Dauchot, J.-L. Thiffeault, and S. Roux. Open-flow mixing: Experimental evidence for strange eigenmodes. *Phys. Fluids*, 21(2):023603, 2009.
- [24] L. Grafakos. *Modern Fourier analysis*. Graduate Texts in Mathematics, 250. Springer-Verlag, New York, third edition, 2014.
- [25] G. Iyer, A. Kiselev, and X. Xu. Lower bounds on the mix norm of passive scalars advected by incompressible enstrophy-constrained flows. *Nonlinearity*, 27(5):973–985, 2014.
- [26] P.-E. Jabin. Critical non-Sobolev regularity for continuity equations with rough velocity fields. *J. Differential Equations*, 260(5):4739–4757, 2016.
- [27] M.-C. Jullien. Dispersion of passive tracers in the direct enstrophy cascade: Experimental observations. *Phys. Fluids*, 15(8):2228–2237, 2003.
- [28] M.-C. Jullien, P. Castiglione, and P. Tabeling. Experimental observation of Batchelor dispersion of passive tracers. *Phys. Rev. Lett.*, 85(17):3636–3639, 2000.
- [29] A. Kiselev and X. Xu. Suppression of chemotactic explosion by mixing. 2015. Preprint. arXiv:1508.05333.
- [30] F. Léger. A new approach to bounds on mixing. 2016. Preprint. arXiv:1604.00907.
- [31] Z. Lin, J.-L. Thiffeault, and C. R. Doering. Optimal stirring strategies for passive scalar mixing. *J. Fluid Mech.*, 675:465–476, 2011.
- [32] W. Liu. Mixing enhancement by optimal flow advection. *SIAM J. Control Optim.*, 47(2):624–638, 2008.
- [33] C. Liverani. On contact Anosov flows. *Ann. of Math. (2)*, 159(3):1275–1312, 2004.
- [34] E. Lunasin, Z. Lin, A. Novikov, A. Mazzucato, and C. R. Doering. Optimal mixing and optimal stirring for fixed energy, fixed power, or fixed palenstrophy flows. *J. Math. Phys.*, 53(11):115611, 2012.
- [35] G. Mathew, I. Mezić, S. Grivopoulos, U. Vaidya, and L. Petzold. Optimal control of mixing in Stokes fluid flows. *J. Fluid Mech.*, 580:261–281, 2007.
- [36] G. Mathew, I. Mezic, and L. Petzold. A multiscale measure for mixing. *Phys. D*, 211(1-2):23–46, 2005.

- 
- [37] J. M. Ottino. *The kinematics of mixing: stretching, chaos, and transport*. Cambridge Texts in Applied Mathematics. Cambridge University Press, Cambridge, 1989.
  - [38] D. Rothstein, E. Henry, and J. P. Gollub. Persistent patterns in transient chaotic fluid mixing. *Nature*, 401(6755):770–772, 1999.
  - [39] C. Seis. Maximal mixing by incompressible fluid flows. *Nonlinearity*, 26(12):3279–3289, 2013.
  - [40] H. Triebel. *Theory of function spaces*. Monographs in Mathematics, 78. Birkhäuser Verlag, Basel, 1983.
  - [41] Y. Yao and A. Zlatoš. Mixing and un-mixing by incompressible flows. *J. Eur. Math. Soc. (JEMS)*. To appear. arXiv:1407.4163.

G.A.

Dipartimento di Matematica, Università di Pisa  
largo Pontecorvo 5, I-56127 Pisa, Italy  
e-mail: [giovanni.alberti@unipi.it](mailto:giovanni.alberti@unipi.it)

G.C.

Departement Mathematik und Informatik, Universität Basel  
Spiegelgasse 1, CH-4051 Basel, Switzerland  
e-mail: [gianluca.crippa@unibas.ch](mailto:gianluca.crippa@unibas.ch)

A.L.M.

Department of Mathematics, Penn State University  
324 McAllister Building, State College, PA 16802, USA  
e-mail: [alm24@psu.edu](mailto:alm24@psu.edu)